An-Najah National University

Faculty of Graduate Studies

The Effects of Magnetic and Electric Fields on Donor Impurity States in GaAs Quantum Dot

By

Asmaa Zohair Madhat Yaseen

Supervisor

Prof. Mohammad Elsaid

Co-Supervisor

Dr. Musa Elhasan

This Thesis is Submitted in Partial Fulfillment of the Requirements for the Degree of Master of Physics, Faculty of Graduate Studies, An-Najah National University, Nablus, Palestine.

2018

The Effects of Magnetic and Electric Fields on Donor Impurity States in GaAs Quantum Dot

By

Asmaa Zohair Madhat Yaseen

This Thesis was Defended Successfully on 3/6/2018 and Approved by:

Defense committee members		**Signature**
- **Prof. Mohammad Elsaid**	**(Supervisor)**	**……**
- **Dr. Musa El-Hasan**	**(Co-Supervisor)**	**……...**
- **Dr. Rezek Estaiteh**	**(External examiner)**	**……**
- **Dr. Muna Hajj Yahya**	**(Internal examiner)**	**……**

Dedication

For my wonderful family for their love, care and support.

Acknowledgments

First and foremost, praises and thanks to the God, for his showers of blessings throughout my thesis work and in each moment in my life.

Secondly, I would like to express my gratitude and appreciation to all those who gave me the possibility to complete this thesis. A special thanks to my supervisor and instructor Prof. Mohammad Elsaid for his guidance, assistance, supervision and contribution of valuable suggestions. Not only the thesis methodologies but also many other suggestions and encouragement. In addition, I would like to thank Dr. Musa Elhasn for his efforts and time. I can't forget to thank Mr. Ayham Shaer for his help and experience especially in Mathematica.

Last but not least I want to take the opportunity, to express a sense of gratitude and love to my especial family, wonderful friends, my work manager and colleagues, and my great students for their moral support and care until the end.

الإقرار

أنا الموقع أدناه مقدم الأطروحة التي تحمل عنوان:

The Effects of Magnetic and Electric Fields on Donor Impurity States in GaAs Quantum Dot

أقر بأن ما اشتملت عليه هذه الرسالة إنما هو نتاج جهدي الخاص، باستثناء ما تمت الإشارة إليه حيثما ورد، وأن هذه الرسالة ككل أو جزء منها لم يقدم من قبل لنيل أية درجة أو بحث علمي أو بحثي لدى أية مؤسسة تعليمية أو بحثية أخرى

Declaration

The work provided in this thesis, unless otherwise referenced, is the researcher's own work, and has not been submitted elsewhere for any other degree or qualification.

Student's name: **اسم الطالب:**

Signature: **التوقيع:**

Date: **التاريخ:**

Table of Contents

List of Tables

List of Figures

List of Symbols and Abbreviations

QD	Quantum Dot
GQD	Gaussian Quantum Dot
PQD	Parabolic Quantum Dot
3D	Three Dimensions
2D	Two Dimensions
1D	One Dimension
0D	Zero Dimension (Quantum Dot)
M	Magnetization
χ	Magnetic Susceptibility
ω_0	Confinement Potential Frequency
ω_c	Cyclotron Frequency
F	Electric Field
B	Magnetic Field
GaAs	Gallium Arsenide
n- AlGaAs	n- type Aluminum Gallium Arsenide
2DEG	Two Dimensional Electron Gas
e	Charge of the Electron
m_0	Mass of the Electron
m^*	Effective Mass of the Electron
$\vec{P}(r)$	The linear Momentum
$\vec{A}(r)$	Vector Potential
c	Speed of Light
$V_c(r)$	Confining Potential
ϵ	The Dielectric Constant of the Material
R^*	Effective Rydberg Energy Unit
$\hbar$	Reduced Plank's Constant

i	Imaginary Number
Φ	Wave Function
K	Kelvin Degree
T	Temperature
n	Principle quantum number
r	Position Coordinate
V_{eff}	Effective potential
L_z	Orbital Angular Momentum in z –Direction
k_B	Boltzman Constant
N	Spatial Dimension
a	Shift parameter
m_l	Angular quantum number
$\bar{k}$	Shifted Variable
E	Energy
n_r	Radial Quantum Number
a^*	Effective Bohr Radius
l	Orbital Quantum Number
$\widehat{H}$	Hamiltonian
LED	Light Emitting Diode
LCD	Liquid Crystal Display

The Effects of Magnetic and Electric Fields on Donor Impurity States in GaAs Quantum Dot

By

Asmaa Zohair Madhat Yaseen

Supervisor

Prof. Mohammad Elsaid

Co-supervisor

Dr. Musa El-Hasan

Abstract

The effects of magnetic and electric fields on the donor impurity states confined in a GaAs two dimensional (2D) parabolic quantum dot has been studied. The impurity energy and binding energy of the ground state and some low-lying excited states were calculated. The Hamiltonian was solved using 1/N expansion method within the effective mass approximation. The results had been displayed as a function of physical parameters: confinement strength ω_0, magnetic field strength ω_c, and electric field strength F.

In addition, we have studied the magnetic properties of the donor impurity in the quantum dot by calculating the magnetization and the magnetic susceptibility. The dependence of the magnetization and the magnetic susceptibility quantities on temperature, confinement strength ω_0, magnetic field ω_c, and electric field strength F were investigated. The comparisons show that our results are in very good agreement with reported works

Chapter One
Introduction

1.1 Low Dimensional Systems

A low dimensional system is one where the motion of electrons is restricted from exploring the full three dimensions of our space. There has been great interest in low dimensional quant um systems within the last two decades for their importance in theoretical physics and practical applications.

So how are electrons restricted from moving in three dimensions? The answer is the quantum confinement effect in the heterostructure materials [1]. Quantization effects become very important when at least one of the three dimensions of semiconductor structure reduced to a length smaller than the Fermi wavelength (generally in the range from 1nm to 100nm) [2-3].

Low-dimensional structures are usually classified according to the number of reduced dimensions they have. More precisely, the dimensionality refers to the number of degrees of freedom for the particle momentum. Based on the confinement direction, a quantum confined structure will be classified into four categories as bulk structure, quantum well, quantum wire and quantum dot [4].

In Three-dimensional (3D) structure or bulk structure: charge carriers (electrons and holes) act free in the three spatial dimensions. In Two-dimensional (2D) structure or quantum well: charge carriers are confined in one direction, while the carriers are free to move in the other two

directions. One-dimensional (1D) structure or quantum wire are formed when two dimensions of the system are confined, leading to free movement along only one direction. Eventually Zero-dimensional (0D) structure or quantum dot confine the charge carriers in all three dimensions [5-6].

As more number of dimensions are confined, more discrete energy levels can be found. The discrete structure of energy levels leads to a discrete absorption spectrum, which is in contrast to the continuous absorption spectrum of a bulk semiconductor. Density of electron states in bulk, 2D, 1D and 0D semiconductor structure is shown in Figure (1.1). 0D structures have very well defined and quantized energy levels [7].

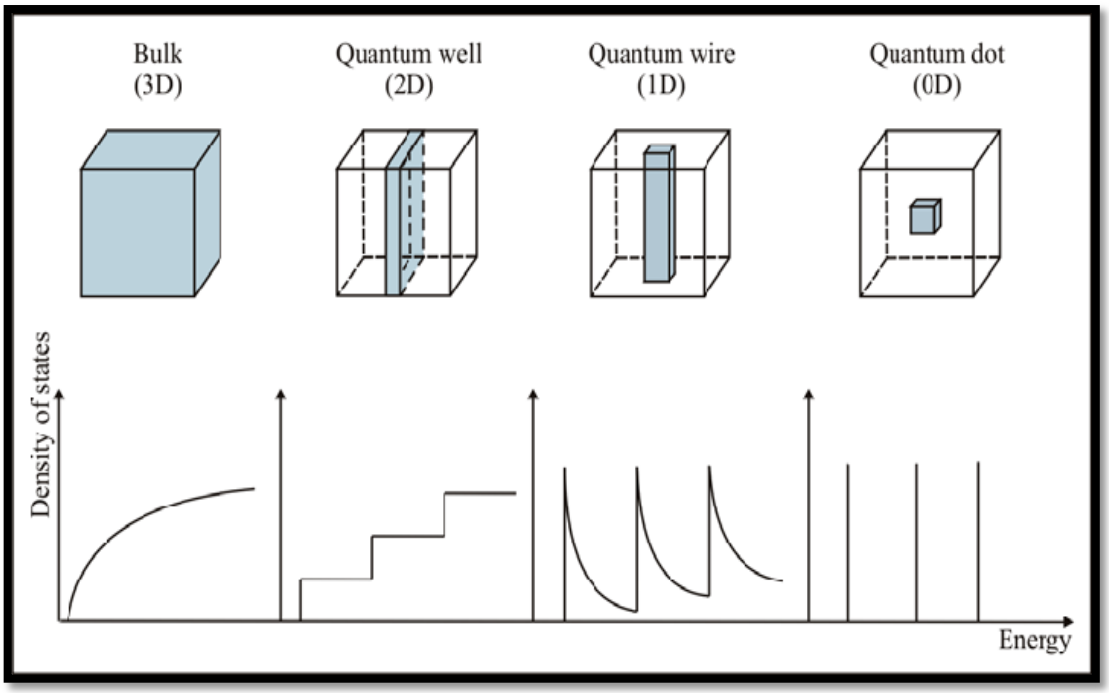

Figure (1.1): Density of states as function of energy for various confinement Systems: bulk materials (3D), quantum well (2D), quantum wire (1D), and quantum dot (0D).

1.2 Quantum Dots

Quantum dots (QDs) were discovered in solids (glass crystals) in 1980, are zero dimensional nanostructures made from semiconductor materials (like GaAs/AlGaAs), in which charge carriers (electrons and holes) are confined in all three spatial dimensions. Due to this confinement the electron states are fully quantized into discrete and narrow electronic energy levels [8-10].

The electronic properties of quantum dots are closely related to their size shape and composition. This allows properties such as the band gap, optical emission color and absorption spectrum to be highly tunable, as the size distribution of quantum dots can be controlled during fabrication. For example, the band gap in a quantum dot, which determines the frequency range of emitted light, is inversely related to its size [11]. Bigger dots emit longer wavelengths like red, while smaller dots emit shorter wavelengths like blue. This property suggests the potential for higher performance and more efficient light emitting diodes (LEDs), displays, and lasers [12].

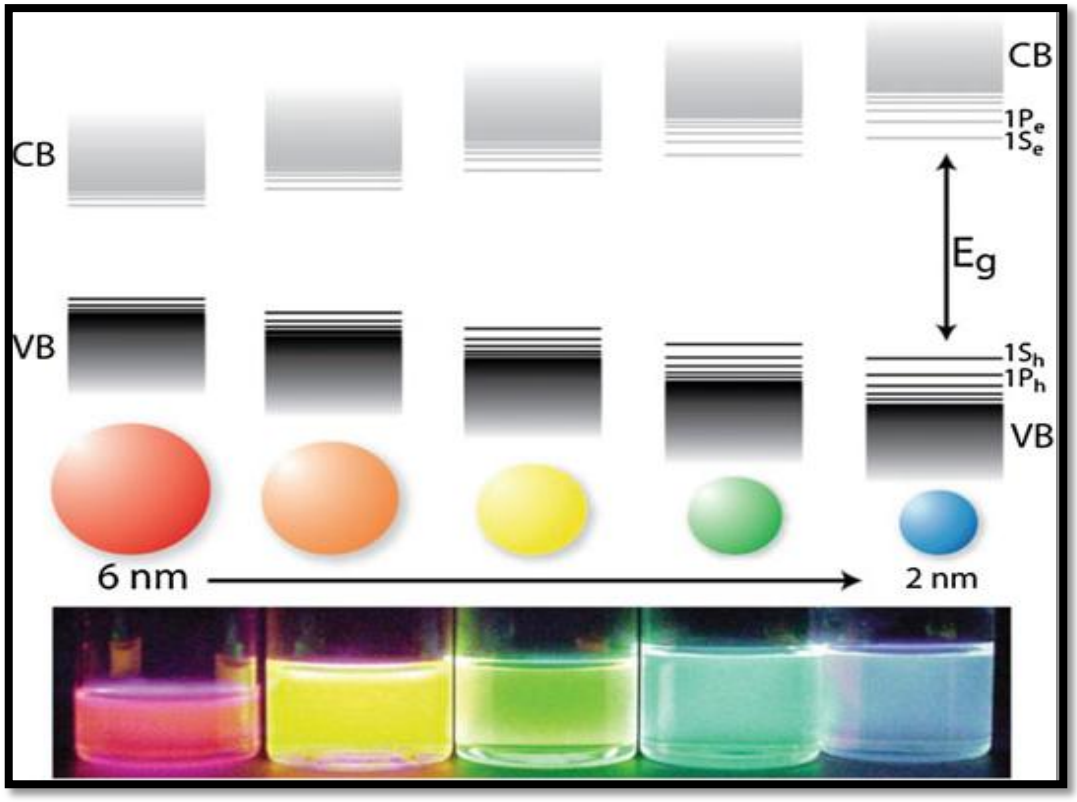

Figure (1.2): Example of size-dependent fluorescence spectra of different colors for quantum dots [13].

Because of the similarity between real atoms and quantum dots, quantum dots are often called the artificial atoms. Both have discrete energy levels and contain a small number of electrons. Electrons in both real and artificial atoms are attracted to a central potential, in a real atom this is a positively charged nucleus (coulomb potential). While in artificial atom these electrons trapped in a bowl like parabolic potential.

The number of electrons in QD's can be controlled by artificial external potential whereas in real atoms by ionization. Moreover, the structure of real atoms is three–dimensional, while most of the artificial quantum dots can be regarded as large 2D atoms, since the lateral dimensions are in most cases much larger than the vertical extension. Which mean that the

number of electrons needed to fill each shell is different from real atoms. Figure (1.3) shows a very schematic comparison of a real three-dimensional atom and a disk-shaped quantum dot [14].

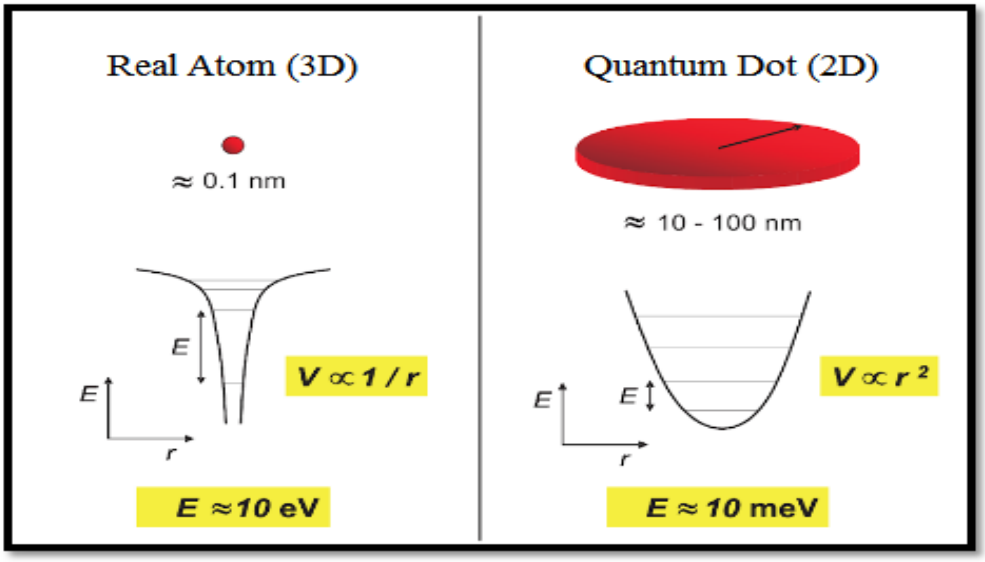

Figure (1.3): a schematic comparison of a real three-dimensional atom and a disk-shaped quantum dot.

QDs had been the subject of interest research due to its many important applications, from lighting and optical applications to use in quantum computing and biological applications.

QDs are being used for all sorts of applications where the control of colored light is important. The easily tunable band gap of quantum dots allows for relatively monochromatic light emission with pure and saturated color. A thin filter made of quantum dots has been developed so it can fit on top of a fluorescent or led lamp particularly for increasing the red emission [15].

There is an active interest in the use of quantum dots in computer screens and displays because they offer many important advantages, conventional LCD use color filters (red, green and blue crystals) that illuminated from behind by a very bright backlight this white light passed through color filters to create the desired color pixel, since much of the light spectrum is absorbed by the filters, energy efficiency is not optimized. In contrast quantum dot display use quantum dot instead of these filters these quantum dots can be tuned to give the light of any color of the spectrum so the colors of a quantum dot display are likely to be much more realistic, moreover, quantum dots produce light themselves so they need no backlight making them much more energy efficient. Finally, quantum dot is much smaller than liquid crystals so they would give a much higher resolution image [16].

1.3 Literature survey

The study of impurities in semiconductor quantum dots (QDs) has attracted much attention in recent years, because of the fact that their presence can dramatically affect the performance of semiconductor devices and their electrical, optical and transport properties.

The investigations of impurity states in semiconductor nanostructures can date back to the early 1980s by Bastard [17]. In spite of growing interest in the topic of impurity doping in nanocrystallites, A great number of theoretical and experimental works have been devoted for understanding the energy levels of donor impurities in low dimensional semiconductor

QDs [18-21], for example Kostic and Stojanovic have investigated the states of a center donor impurity in a spherical CdTe/ZnTe QD using a spherically confining potential of finite depth [22].

The binding energy of donor impurities in QD's depends on materials, geometry, size, and shape. The impurity binding energy may strongly depend on the position of the impurity along the heterostructures as well as on the typical dimensions of the heterostructures. In particular, Perez-Merchancano et al. [23] and Zhu et al. [24] made the first studies about the confinement effects on the impurity states in QDs. They calculated binding energies for the ground and excited states as a function of dot size and the impurity position. Xie [25] and Zhu et al. [26] have investigated the binding energy of hydrogenic donor impurity in a parabolic quantum dot using diagonalization method.

Calculations of the binding energy of an on-center and off-center shallow hydrogenic impurity in a GaAs quantum dot under hydrostatic pressure were carried out in 2007 by Perez-Merchancano and Bolivar-Marinez using variational approach [27].

As the state of charge carrier's change in the presence of hydrogenic impurity, it also changes in the presence of electric and magnetic fields. External fields are effective tools for studying the properties of impurities in semiconductor QD's. The effects of an applied magnetic and electric fields of arbitrary strength on the energy and binding energy of donor impurity in a quantum dot had been studied by many authors using

different computational approaches [28-31]. Elsaid had used 1/N expansion method to calculate the energy states of an electron bound to the donor impurity in the presence of a magnetic field of arbitrary strength [32].

The combination effects of the electric and magnetic fields on the binding energy of an on-center donor impurity in disc-shaped GaAs/Al0.3Ga0.7As quantum dots was studied by Zaiping Zeng et al in 2014 [33].

In 2004 John Peter and coworkers have used a variational method for the calculations of the electric and magnetic fields on the binding energies of hydrogenic donors in a parabolic diluted magnetic semiconductor QD [34]. Rezaei and kish had applied the direct matrix diagonalization method to study the electric and magnetic field effects on a hydrogenic donor impurity confined in a 2D parabolic quantum dot [35].

Boda and Chatterjee studied the transition energies and magnetic properties of a neutral donor complex in a Gaussian GaAs QD in the presence of an external magnetic field in 2016[36].

The binding energies of the ground state of a hydrogenic impurity in a GaAs QD dots subjected to external electric and magnetic fields have been calculated by Zhang Hong, Zhai Li-Xue, Wang Xue, Zhang Chun-Yuan and Liu Jian-Jun using the finite-difference method [37].

J-H Yuan et al. investigated theoretically the low-lying states and optical absorption properties of a hydrogenic impurity in a parabolic QD

modulation by the applied electric field. Bzour searched in the effects of hydrostatic pressure and temperature on the properties of the GaAs single QD in an external magnetic field with the help of exact diagonalization technique [39]. In 2015 Shaer studied the heat capacity of two electrons QD in an external magnetic field by using variational method [40]. Very recently, Elsaid et al. had used variational and exact diagonalization methods to study the electronic, thermodynamic and magnetic properties of single and coupled QDs [41-46].

1.4 Research Objectives

This work has two main objectives, which can be summarized as follows;

1- We have employed the shifted 1/N expansion method to solve the QD Hamiltonian and then to obtain the energies (eigenvalues) of the donor impurity in a parabolic confinement in an external electric and magnetic field of arbitrary strength. The complete energy spectra of the system were calculated as a function of magnetic field strength (ω_c), confinement strength (ω_0), and electric field strength (F).

2- We have used the computed (eigenenergies) to calculate the magnetic properties of the donor impurity like the magnetization (M) and the magnetic susceptibility (χ) quantities.

1.4 Thesis Layout.

In this work, the donor impurity energy and binding energy for the ground state and low-lying excited states of GaAs quantum heterostructure had been calculated as a function of the confinement strength ω_0, magnetic field strength ω_c, and electric field strength F. The shifted 1/N expansion method has been used to solve the QD Hamiltonian to obtain the eigenvalues. Then, the magnetization and the magnetic susceptibility had been investigated as a magnetic property of the QD system, the magnetization and the magnetic susceptibility were calculated as a function of the magnetic field strength ω_c at different values of the temperature T, confinement strength ω_0 and electric field strength F.

The rest of this thesis is organized as follows: the donor impurity Hamiltonian, the principle of shifted 1/N expansion technique and how to calculate the magnetization and the magnetic susceptibility from the statistical energy expressions are presented in chapter two, in chapter three the results of energy, binding energy, magnetization and magnetic susceptibility has been displayed and discussed. The final chapter devoted to conclusions and future work.

Chapter Two
Theory

The model and the method used for our calculations will be discussed in details in this chapter. So the three main parts are: quantum dot Hamiltonian, the shifted 1/N expansion method, and the magnetic properties of the donor impurity in the quantum dot.

2.1 Donor Impurity Hamiltonian

Our model consists of a system of one electron with effective mass (m^*) and charge (e), moving in a two dimensional (2D) parabolic quantum dot (PQD) (like a disc) under the effects of external uniform electric and magnetic fields, in the presence of a center donor impurity. The Hamiltonian of the impurity in a parabolic QD is given as:

$$\widehat{H} = \frac{1}{2m*}(\vec{P} + \frac{e}{c}\vec{A})^2 - \frac{e^2}{\varepsilon r} - eFr + V_c(r) \quad (1)$$

$\vec{P}$ refers to the electron momentum operator corresponding to the electron position coordinate $r(x, y)$. $\vec{A}$ is the magnetic vector potential which is related to the applied magnetic field $\vec{B}$ by $\vec{B} = \nabla \times \vec{A}$. The vector potential is chosen to be in the symmetric gauge as $\vec{A} = \frac{B}{2}(-y, x, 0)$, B is assumed to be uniform and normal to the 2D QD plane along the z-axis. ε represented the dielectric constant of GaAs quantum dot, c is the speed of light, and F is the strength of the electric field in the radial direction.

Finally, $V_c(\mathrm{r})$ is the confining potential:

$$V_c(\mathrm{r}) = \frac{1}{2} m^* {\omega_0}^2 r^2 \tag{2}$$

In which ω_0 is the strength of the confinement potential frequency.

Now, the Hamiltonian of the system Eq. (1) is:

$$\widehat{H} = \frac{1}{2m*}\left[\vec{\mathrm{P}}.\vec{\mathrm{P}} + \frac{e^2}{c^2}\vec{\mathrm{A}}.\vec{\mathrm{A}} + \frac{2\mathrm{e}}{C}\vec{\mathrm{A}}.\vec{\mathrm{P}}\right] - \frac{e^2}{\varepsilon \mathrm{r}} - eFr + \frac{1}{2} m^* \omega_0^2 r^2$$

$$\widehat{H} = \frac{1}{2m*}\left[-\hbar^2\nabla^2 + \frac{e^2}{c^2}\frac{B^2 r^2}{4} + \frac{2\mathrm{e}}{C}\frac{B}{2}\left(xP_y - yP_x\right)\right] - \frac{e^2}{\varepsilon \mathrm{r}} - eFr + \frac{1}{2} m^* \omega_0^2 r^2$$

$$\widehat{H} = \frac{-\hbar^2}{2m*}\nabla^2 + \frac{1}{8} m^* \omega_c^2 r^2 + \frac{1}{2}\omega_c L_z - \frac{e^2}{\varepsilon \mathrm{r}} - eFr + \frac{1}{2} m^* \omega_0^2 r^2$$

$$\widehat{H} = \frac{-\hbar^2}{2m*}\nabla^2 + \frac{1}{2} m^* \Omega^2 r^2 + \frac{\omega_c}{2} m_l \hbar - \frac{e^2}{\varepsilon r} - eFr \tag{3}$$

L_z symbolized the orbital angular momentum for the electron along the z-direction with eigenvalue $m_l\hbar$, $m_l = 0, \pm 1, \pm 2$ is the magnetic quantum number.

$\Omega = (\omega_0^2 + \frac{\omega_c^2}{4})^{\frac{1}{2}}$ is the effective frequency depends on both the magnetic field cyclotron frequency $(\omega_c = \frac{\mathrm{eB}}{m^* c})$, also on the confinement frequency ω_0.

Throughout this work we will use the effective Rydberg $R_y^* = \frac{m^* e^4}{2\varepsilon^2 \hbar^2}$ as the unit of energy and the effective Bohr radius $a_B^* = \frac{\varepsilon \hbar^2}{m^* e^2}$ as the unit of length. In these dimensionless effective units the Hamiltonian assumes the form:

$$\widehat{H} = -\nabla^2 + \frac{1}{4}\Omega^2 r^2 + \frac{\omega_c}{2} m_l - \frac{2}{\varepsilon r} - Fr \tag{4}$$

We have applied the shifted 1/N expansion technique to solve the above Hamiltonian Eq. (4) and obtained the eigenenergies.

2.2 Shifted 1/N Expansion Method

The shifted 1/N expansion method is a powerful technique to solve Schrodinger equation for spherically symmetric potential V(r); it produces exact results for the harmonic oscillator and for the Coulomb potential cases.

The technique is quite simple and it gives an accurate result. Its starts by writing radial Schrodinger equation in N spatial dimensions as:

$$[-\ (\frac{d^2}{dr^2} + \frac{N-1}{r}\ \frac{d}{dr}\ ) + \frac{l(l+N-2)}{r^2} + V(r)]\ \phi(r) = E\ \phi(r) \qquad (5)$$

Where

$$V(r) = -\frac{2}{r} + \frac{1}{4}\Omega^2 r^2 + \frac{\omega_c}{2} m_l - Fr \qquad (6)$$

$l(l+N-2)$ is the eigenvalue of the square of the orbital angular momentum operator in N dimension space and $l = |m_l|$.

The main idea of the shifted $1/N$ expansion method is to rewrite Eq. (5) by using a parameter k , $k = N + 2l$ and a suitable shift parameter a.

In terms of the shifted variable, $\bar{k} = k - a$ one has:

$$[-\frac{d^2}{dr^2} + \bar{k}^2(\ \frac{[1-(1-a)/\bar{k}][1-(3-a)/\bar{k}]}{4r^2}\ + \frac{V(r)}{Q}\ )]\ \phi(r) = \mathrm{E}\ \phi(r) \qquad (7)$$

Where Q is a scaling constant to be determined later. For large $\bar{k}$, the main contribution to the energy E comes from the effective potential, and the kinetic energy becomes negligible.

$$V_{eff} = \frac{1}{4r^2} + \frac{V(r)}{Q} \tag{8}$$

$V(r)$ is supposed to be well behaved so that V_{eff} has a minimum r_0 given by the relationship:

$$2r_0^3 V'(r_0) = Q \tag{9}$$

It is appropriate to shift the origin of coordinates to the position of the minimum (r_0) of the effective potential (V_{eff}) by defining a new variable x.

$$x = \frac{\bar{k}^{1/2}}{r_0}(r - r_0) \tag{10}$$

If Eq. (7) expands around r_0 (respectively $x = 0$) an analytical equation similar to the Schrodinger equation of the one dimensional anharmonic oscillator is found. So it is easy to compare the coefficients of both equations to define all the anharmonic oscillator parameters in terms of $\bar{k}$, Q, r_0 and the potential derivatives in order to obtain the energy spectrum. (See Appendix)

For any value of n_r (radial quantum number) and for any value of m_l the energy $E\ (n_r\ , m_l)$ is given by an expression in powers of $1/\bar{k}$ (up to third order) as:

$$E = E_0 + E_1 + E_2 + E_3 \tag{11}$$

Where E_0, E_1, E_2, E_3 are given in Appendix.

The shift parameter a is chosen so as to make E_1 vanishes. So,

$$a = 2 - (2n_r{+}1)\,\omega \tag{12}$$

ω is the anharmonic oscillator frequency given in Appendix. (Equation A.4).

The constant Q chosen such as to make Eqs. (5) and (7) equals. This means:

$$\bar{k} = \sqrt{Q} \tag{13}$$

By using Eqs. (9), (equation A.4), and (12), an equation for determining the root (r_0) is given below:

$$\left(2r_0^3 V'(r_0)\right)^{1/2} = 2 + 2l - 2 + (2n_r + 1)\left[3 + \frac{r_0 V''(r_0)}{V'(r_0)}\right]^{1/2} \tag{14}$$

With this value of r_0, one can determine ω, a and every identified parameters, which completes all necessary steps to compute the energy eigenvalues of $V(r)$.

By substituting the applied potential $V(r)$ in Eqs. (9), (14), (Equation A4) we get:

$$Q = 4r_0 + \Omega^2 r_0^4 - 2Fr_0^3 \tag{15}$$

$$\{4r_0 + \Omega^2 r_0^4 - 2Fr_0^3\}^{1/2} = 2 + 2l - 2 + (2n_r + 1)\left\{3 + \frac{\left(-4/r_0^2 + \Omega^2 r_0/2\right)}{\left(2/r_0^2 + \Omega^2 r_0/2 - F\right)}\right\}^{1/2} \tag{16}$$

$$\omega = \left(3 + \frac{\left(-4/r_0^2 + \bar{\omega}^2/2r_0\right)}{\left(2/r_0^2 + \bar{\omega}^2 r_0/2\right)}\right)^{1/2} \tag{17}$$

One can calculate the binding energy (EB) of a hydrogenic donor impurity as:

$$EB = E^0 - E \tag{18}$$

E^0: The eigenvalue of the system without hydrogenic impurity.

E : The eigenvalue of the system with hydrogenic impurity.

2.3 The Magnetic Properties of the Quantum Dot.

The Magnetization (M) of donor impurity can be calculated by differentiating the average statistical energy of the 2D QD system with respect to the magnetic field strength B.

$$M(T, \omega_0, B, F) = -\frac{\partial <E>}{\partial \mathrm{B}} \tag{19}$$

Where $<\mathrm{E}> = \sum_{\alpha=1}^{N} \frac{\mathrm{E}_\alpha e^{-\mathrm{E}_\alpha(\mathrm{B})/k_B T}}{e^{-\mathrm{E}_\alpha(\mathrm{B})/k_B T}}$ (20)

By substituting Eq.(20) in Eq.(19), we can express the magnetization (M) in a common standard from as:

$$M(T, \omega_0, B, F) = -\frac{\sum_{\alpha=1}^{N} \frac{\partial \mathrm{E}_\alpha(\mathrm{B})}{\partial B} e^{-\mathrm{E}_\alpha(\mathrm{B})/k_B T}}{\sum_{\alpha=1}^{N} e^{-\mathrm{E}_\alpha(\mathrm{B})/k_B T}} \tag{21}$$

The magnetic susceptibility (χ), in the presence of the donor impurity, can be obtained by differentiating the magnetization(M) with respect to the magnetic field strength B:

$$\chi = \frac{\partial M}{\partial B} \tag{22}$$

Chapter Three
Results and Discussions

In this chapter we will discuss our computed numerical results for a single donor impurity located at the center of a GaAs two dimensional quantum dot, confined by a parabolic potential of strength ω_0, under the effect of an applied uniform magnetic field of strength ω_c, in addition to a uniform electric field of strength F.

The physical parameters used for GaAs medium in numerical computations are: the effective mass of an electron ($m^* = 0.067m_e$), the dielectric constant of the material (ϵ =12.5), and the effective Rydberg ($R^* = 5.83\ meV$).

3.1 Energy Spectra

In the first stage of our present computational task, we have calculated the ground state energy for the donor impurity of GaAs/AlGaAs QD at various magnetic field values and for two values of the confinement frequency strength ω_0 in the reason of comparison, namely ω_0 =5.412 R^* and $\omega_0 = 3.044\ R^*$, for zero electric field case. The accuracy of our obtained results is compared with previous reported work [32] as shown in Table (3.1). The comparison obviously shows excellent agreement between both works.

Table (3.1): The ground-state energies ($in\ units\ of\ R^*$) at different values of the magnetic field strength (ω_c) and for different values of ω_0, calculated by 1/N expansion method, compared with the reported work Ref [32].

	ω_0 =5.412 R^*		ω_0 =3.044 R^*	
ω_c (R^*)	E(present work) (R^*)	E(Ref[32]) (R^*)	E(present work) (R^*)	E(Ref[32]) (R^*)
2	-2.1197	-2.15	−3.28049	-3.29
4	-1.9704	-2.00	−3.1004	-3.11
6	-1.7343	-1.76	−2.7967	-2.80
10	-1.0454	-1.06	−1.9231	-1.92
18	0.9457	0.93	0.2892	0.28
20	1.5272	1.52	0.9133	0.91

In Figure (3.1) we have shown the effect of the confinement potential frequency ω_0 on the ground state energy of donor impurity for zero electric and magnetic fields. It is clearly seen that: as the confinement strength ω_0 increases, the ground state energy increases also due to the confinement enhancement.

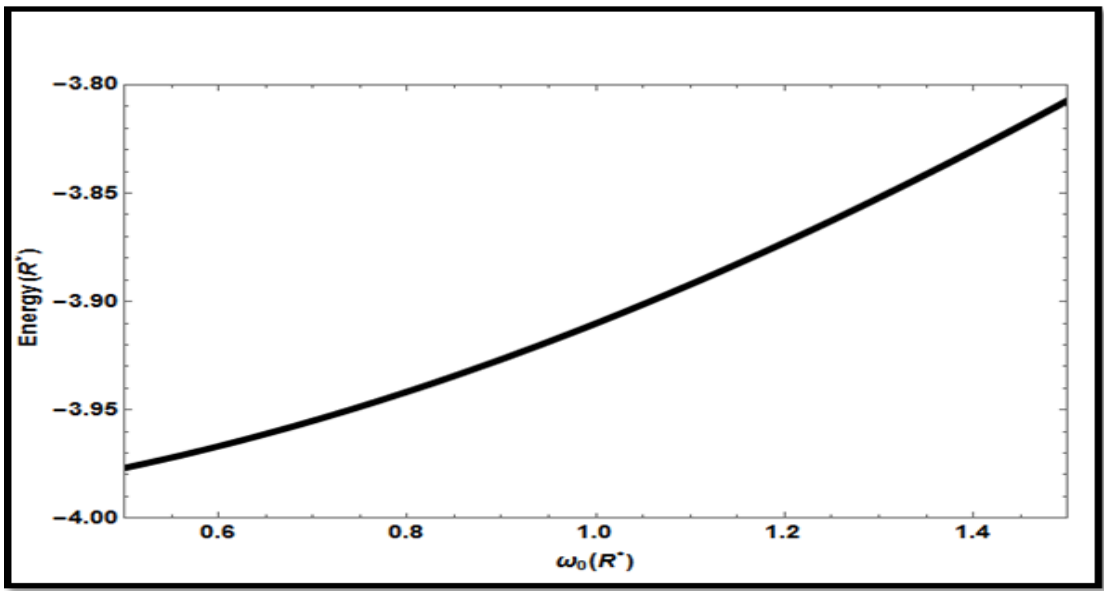

Figure (3.1): The donor impurity ground state energy ($in\ units\ of\ R^*$) as a function of confinement frequency(ω_0), for zero electric and magnetic fields.

In Figure (3.2) we display the ground state energy as a function of the confinement strength ω_0, the solid line indicates the absence of the impurity, and the dashed one indicates the presence of the impurity. The Figure shows a reduction in the energy of the electron because the donor impurity lowers the energy of the heterostructure due to its negative coulomb attraction.

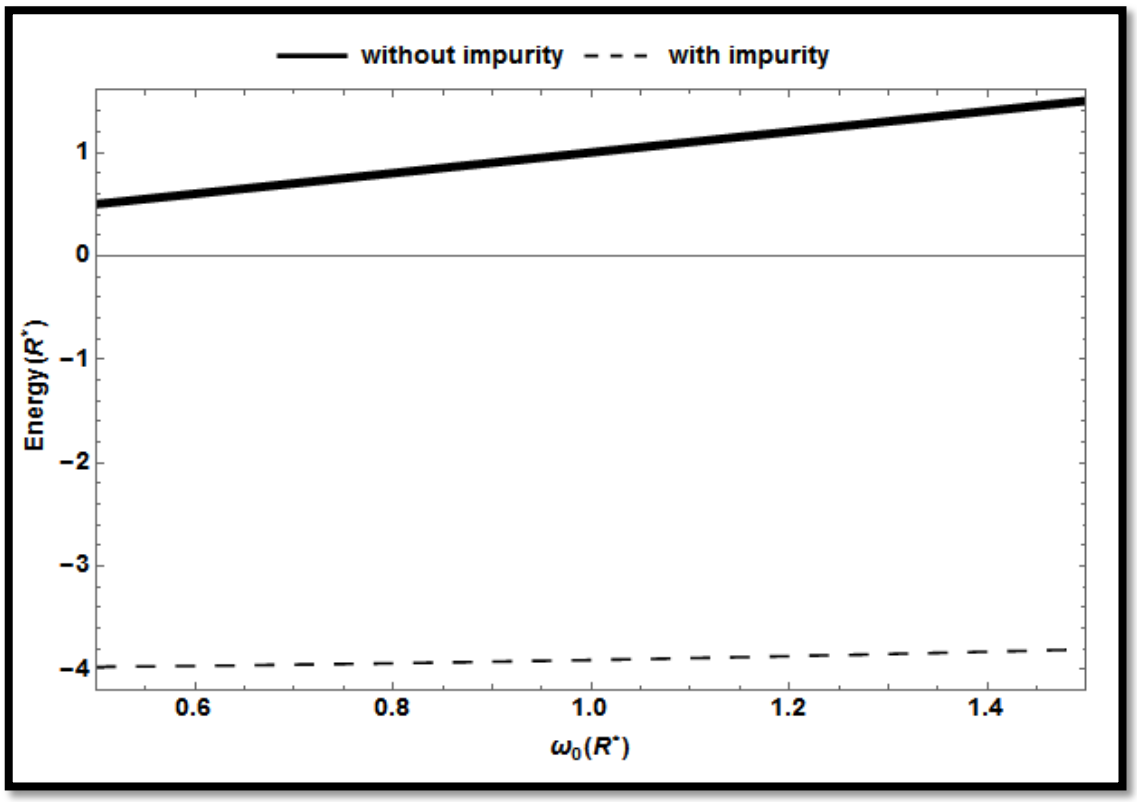

Figure (3.2): The ground state energy of the heterostructure ($in\ units\ of\ R^*$) as a function of confinement strength ω_0 , for zero electric and magnetic fields.

In Figure (3.3) we have shown the energy of low-lying excited states as a function of the confinement strength ω_0 in the presence of the donor impurity, and for zero electric and magnetic fields. As Figure (3.3) clearly shows, the donor impurity energy of these states increases as ω_0 increases

similar to the behavior of the donor impurity energy in the ground state (Figure 3.1).

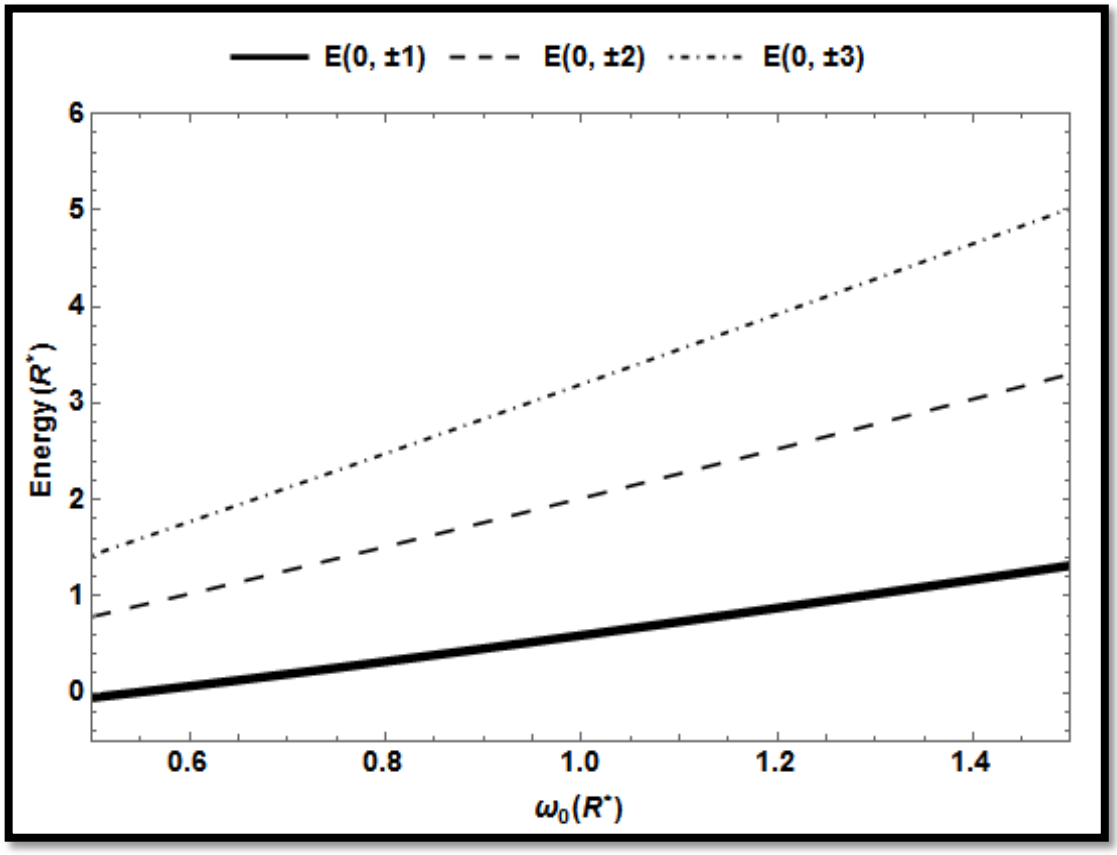

Figure (3.3): The energy for low-lying excited states of the impurity ($in\ units\ of\ R^*$) as a function of the confinement strength ω_0 , for zero electric and magnetic fields.

Figure (3.4) shows the dependence of the ground state binding energy of the impurity on the confinement strength ω_0, for zero electric and magnetic fields. As the Figure clearly shows, the binding energy (BE) increases as ω_0 increases, since the electron becoming more confined toward the center of the quantum dot where the donor impurity resides (coulomb term increases).

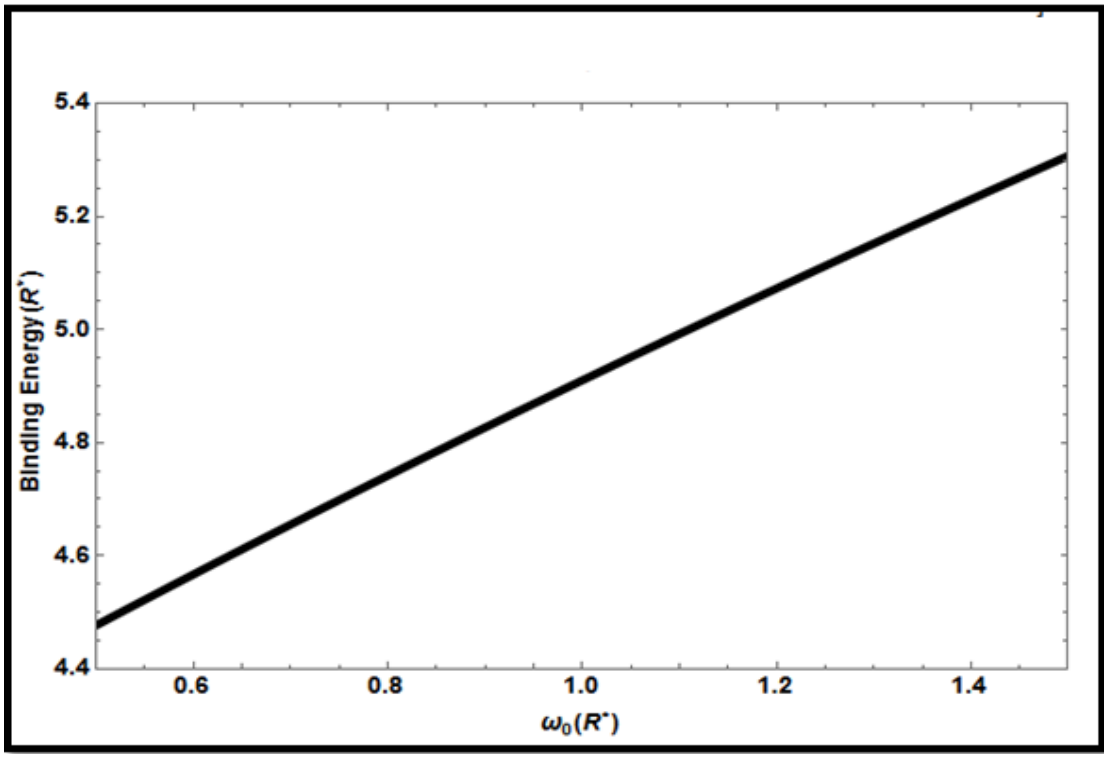

Figure (3.4): The binding energy for the ground state of the impurity ($in\ units\ of\ R^*$) as the function the of confinement frequency ω_0, for zero electric and magnetic fields.

In addition, we have shown the dependence of the binding energy on the confinement strength ω_0 for low-lying excited states as shown in Figure (3.5), in the presence of donor impurity and for zero electric and magnetic fields. As the Figure clearly shows, the binding energy (BE) increases as ω_0 increases, similar to the behavior of the donor impurity binding energy in the ground state (Figure 3.4).

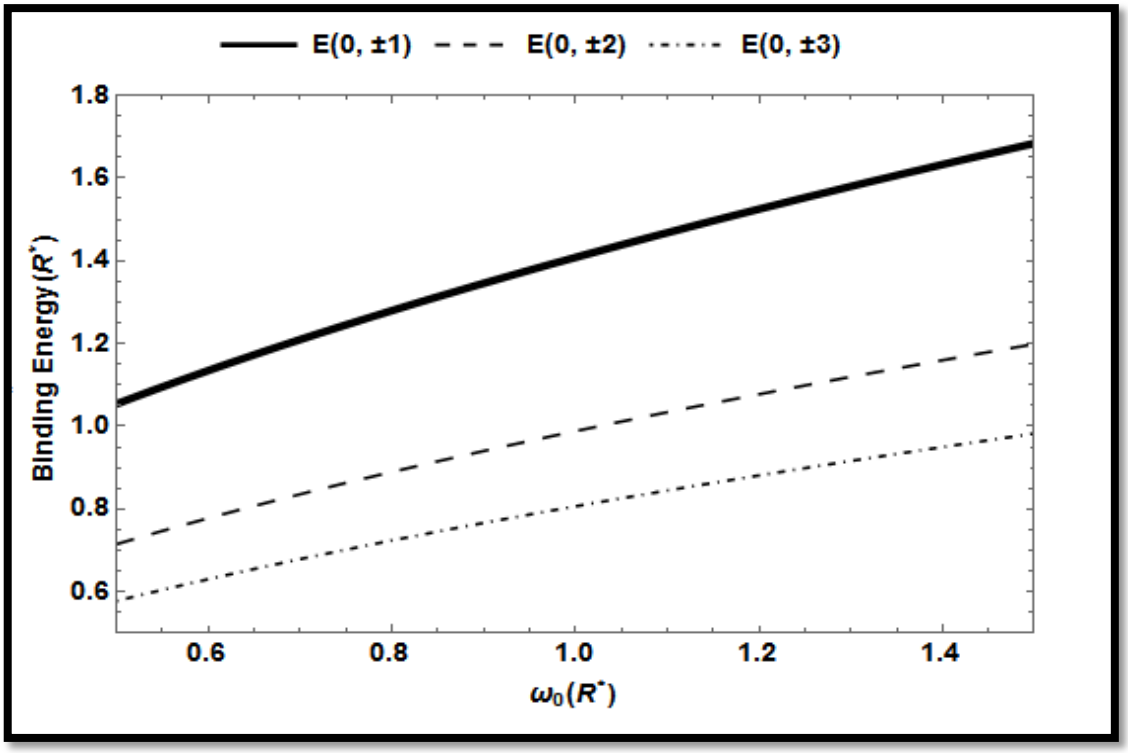

Figure (3.5): The binding energy of the impurity for low-lying excited states ($in\ units\ of\ R^*$) as a function of the confinement strength ω_0, for zero electric and magnetic fields.

3.2 Electric and Magnetic Fields Effects on the Donor Impurity Energy and Binding Energy

In this section, we display the effects of external electric and magnetic fields on the energy and the binding energy for the ground state and low-lying excited states of a donor impurity confined in a GaAs two dimensional PQD.

The dependence of the ground state energy and binding energy of the donor impurity on the magnetic field strength (ω_c) for different values of confinement strength (ω_0) are presented in Figure (3.6) for the energy, and Figure (3.7) for the binding energy, for zero electric field case. It is obvious that both the energy and the binding energy for the ground state of

the impurity increase with the magnetic field because of the increasing compression of the wave function with the magnetic field.

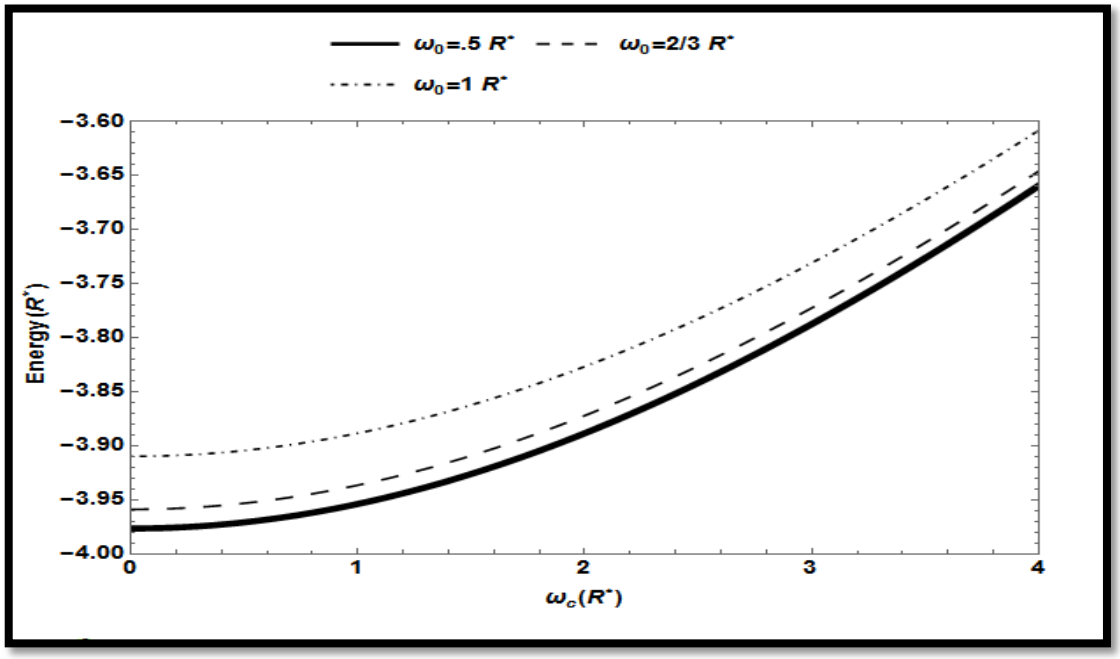

Figure (3.6): The energy for the ground state of the impurity $(in\ units\ of\ R^*)$ as a function of magnetic field of strength ω_c, for three different quantum confinements, and zero electric field.

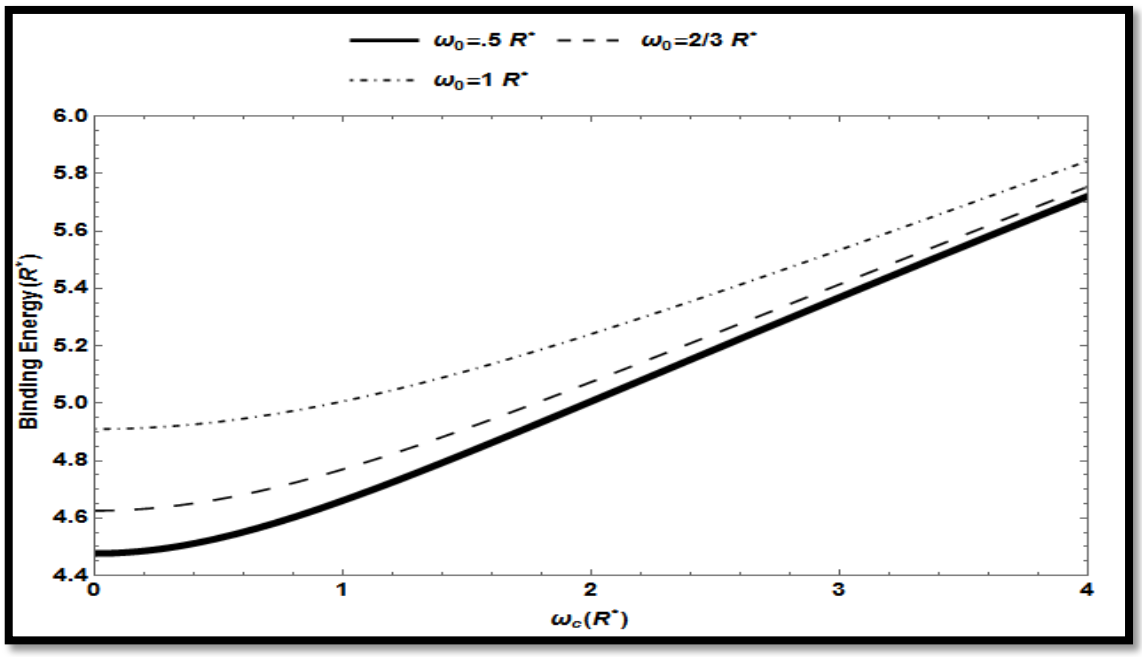

Figure (3.7): The binding energy for the ground state of the impurity $(in\ units\ of\ R^*)$ as a function of magnetic field of strength ω_c, for three different quantum confinements, for zero electric field.

In Figure (3.8) the dependence of the impurity energy on the magnetic field for excited states are presented in the absence of the electric field. It is interesting to note that the degeneracy of the states is removed by applying magnetic field, the energy of $m_r \neq 0$ states is affected not only by the diminished area of localization due to the growth of ω_c , but also due to the addition of the positive or negative (for $m_r = \pm 1, \pm 2, \pm 3$) energy of azimuthal motion of the electron in the magnetic field ($\frac{\omega_c}{2} m_l \hbar$).

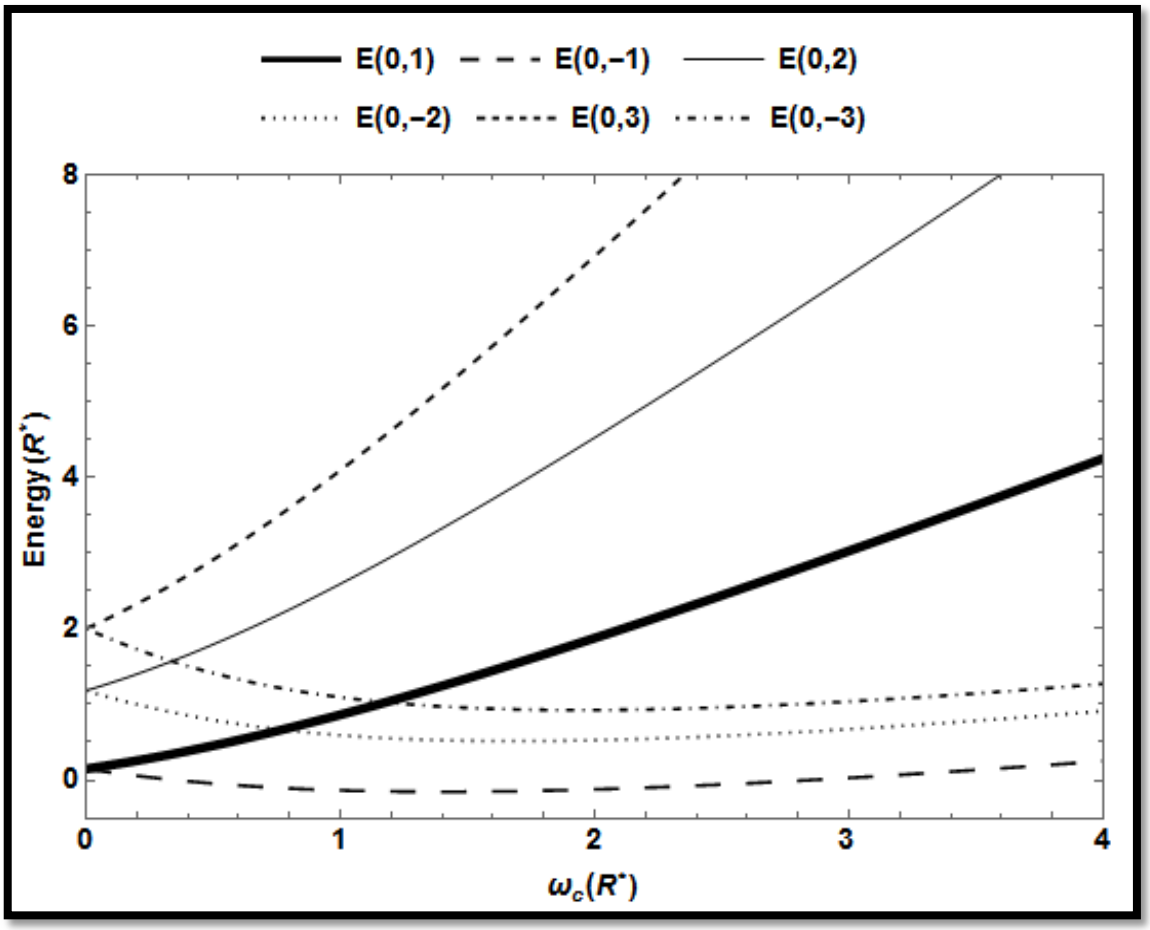

Figure (3.8): The energy for low-lying excited states of the impurity ($in\ units\ of\ R^*$) as a function of the magnetic field of strength ω_c, for $\omega_0 = 2/3R^*$ and zero electric field.

Figure (3.9) and (3.10) show the effect of the electric field on the energy and the binding energy for the ground state of the donor impurity respectively. It is clearly seen that both the energy and the binding energy of the donor impurity decrease with the increase of the electric field(F). With the increase of the electric field, the coulomb potential is more and more weak because of the change of the distribution of the electronic probability density (Increasing the electric field causes the weaker confinement of carriers in the QD. This lead to lower the value of energy).

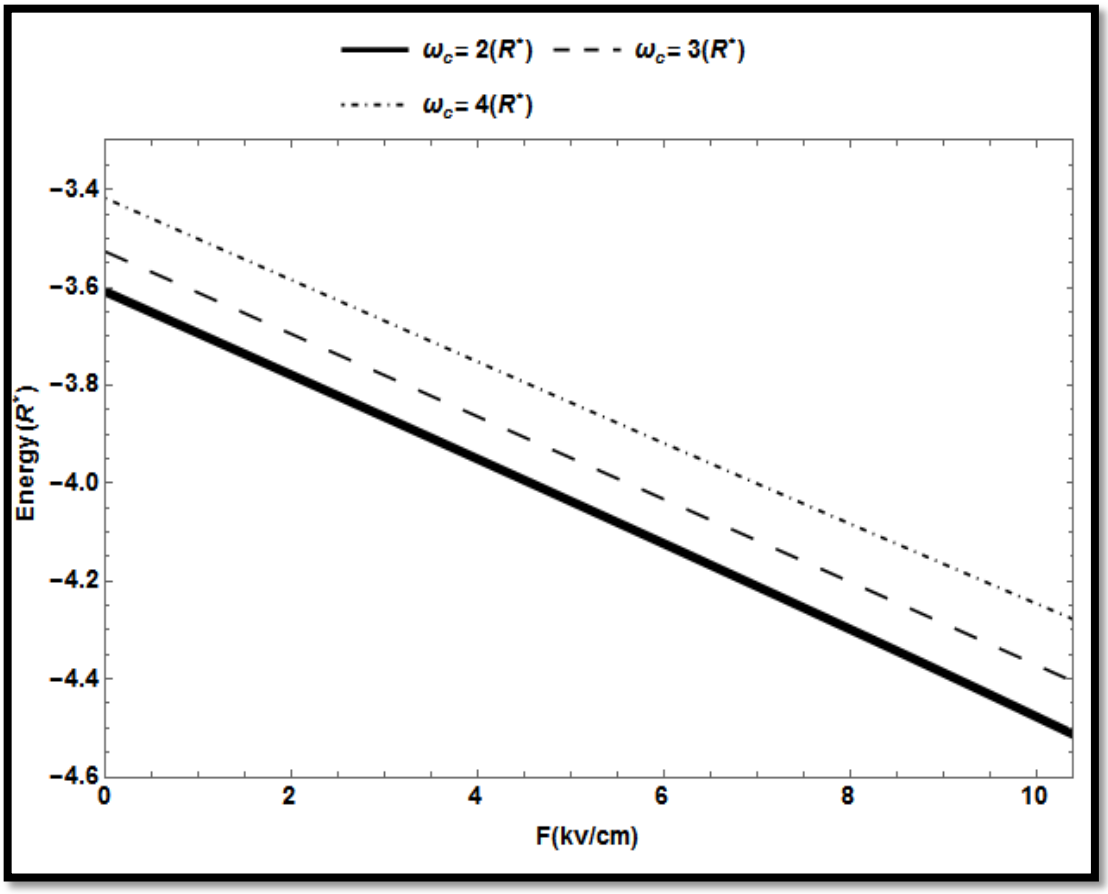

Figure (3.9): The energy for the ground state of the impurity ($in\ units\ of\ R^*$) as a function of the electric field , calculated for various values of $\omega_c,\ and\ \omega_0 = 2\ R^*$.

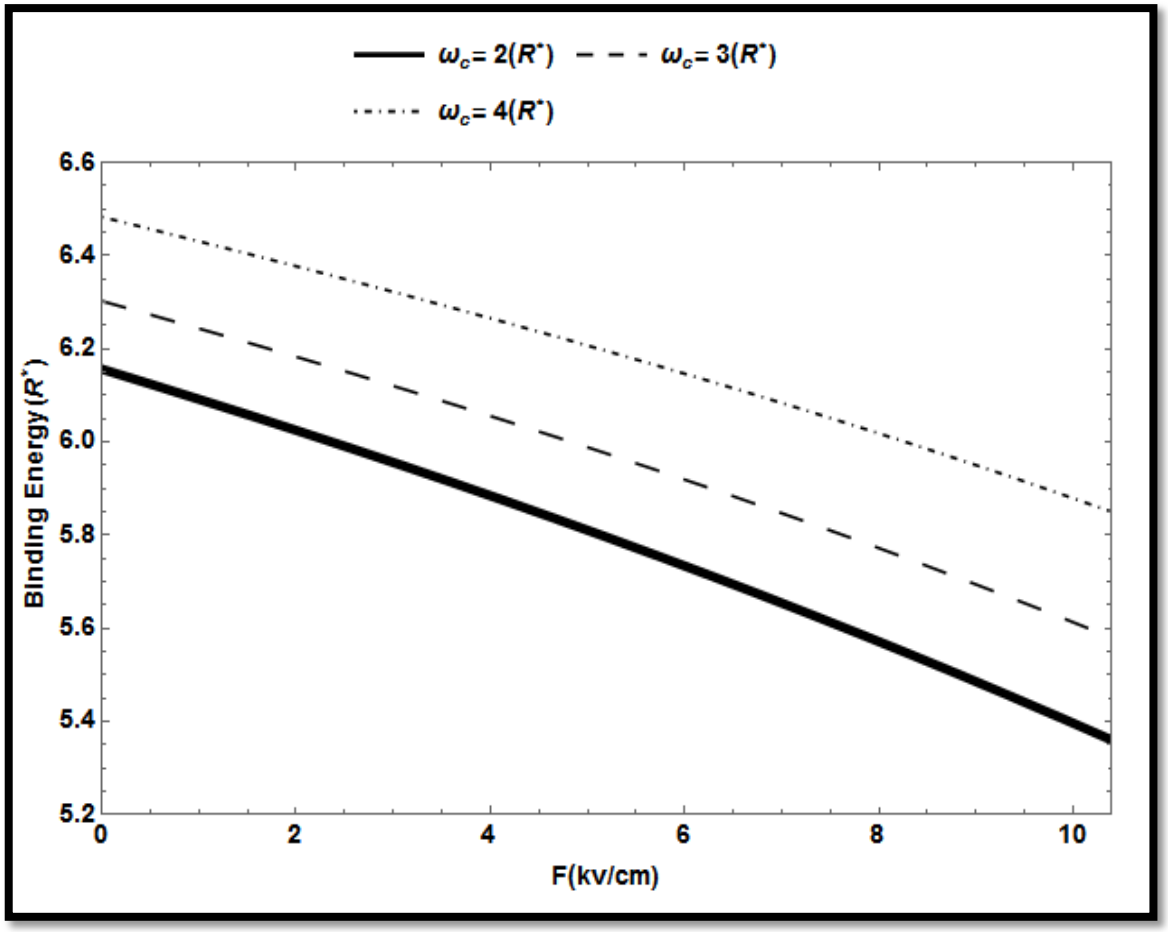

Figure (3.10): The ground state binding energy of the donor impurity ($in\ units\ of\ R^*$) as a function of the electric field , for various values of ω_c, and $\omega_0 = 2.5\ R^*$.

Next, we have calculated the average statistical energy of the QD as shown in Figure (3.11) and Figure (3.12). These Figures show the dependence of the average statistical energy $< E >$ on the magnetic field strength ω_c, for different values of temperature(T), namely $T = 10K$ and $T = 100k$, respectively. The solid line indicates the absence of the impurity, and the dashed one indicates the presence of the impurity, it is clear from the Figures that the effect of the impurity is to decrease the average statistical energy $< E >$ of the system. The presence of donor impurity lowers the energy of the heterostructure due to its negative coulomb attraction.

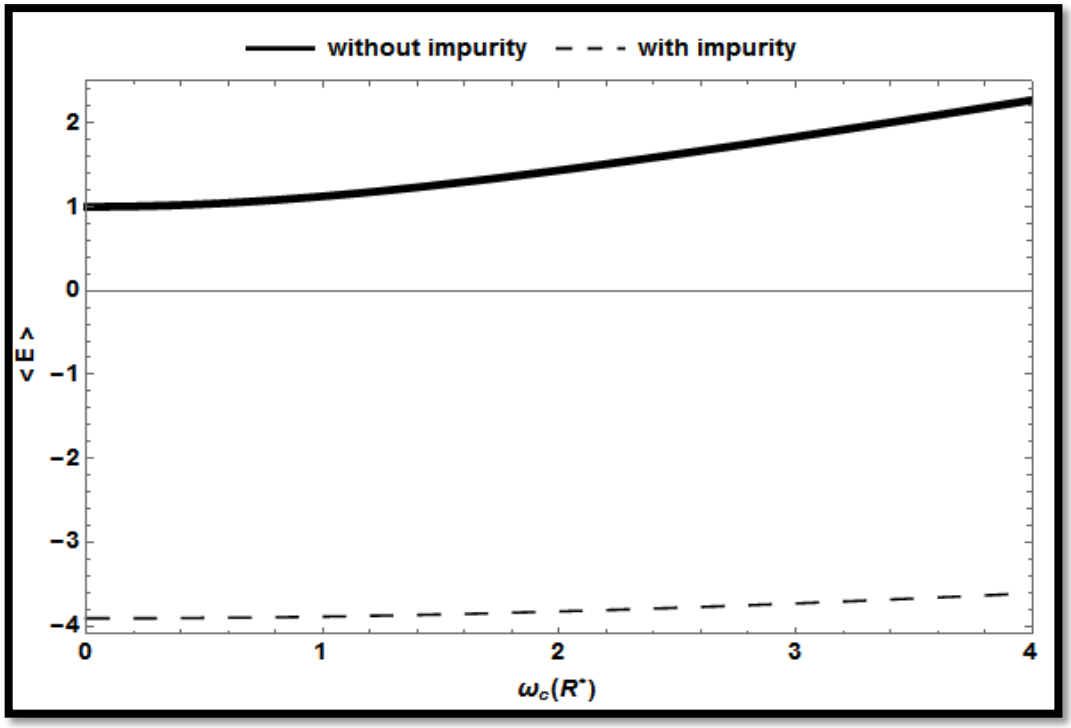

Figure (3.11): The average statistical energy < E > ($in\ units\ of\ R^*$) as a function of the magnetic field of strength ω_c, calculated at: $T = 10K$, $\omega_0 = 1R^*$, and zero electric field.

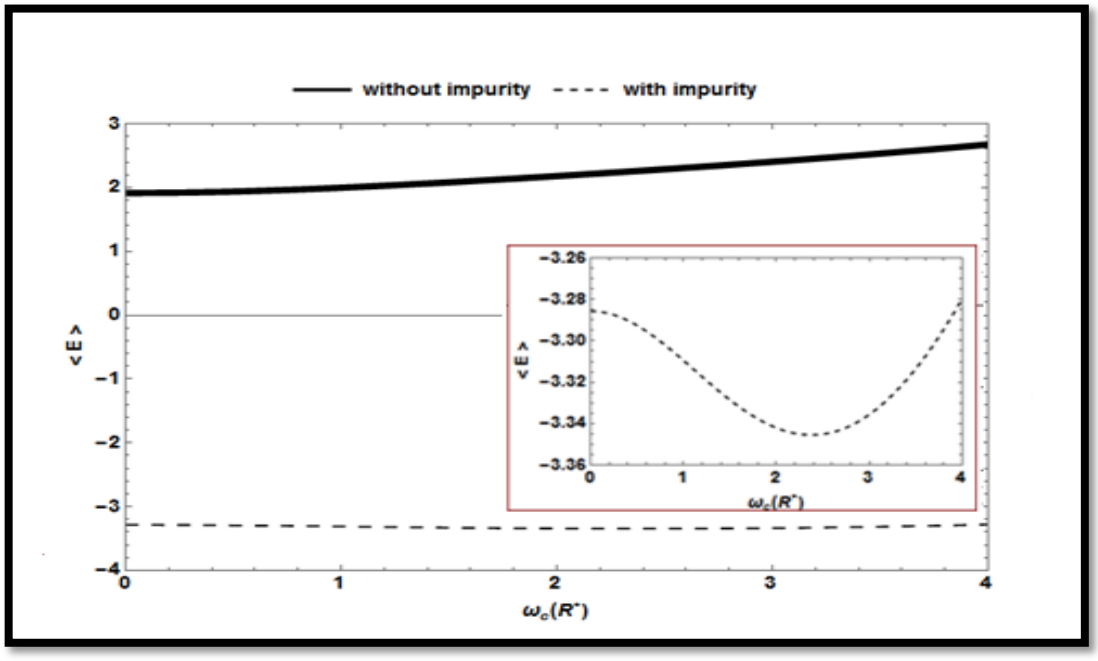

Figure (3.12): The average statistical energy < E > ($in\ units\ of\ R^*$) as a function of the magnetic field of strength ω_c, calculated at: $T = 100K$, $\omega_0 = 1R^*$, and zero electric field. (The inset figure explains the variation of < E > of the system with impurity using small step in energy).

Figure (3.13) describes the average statistical energy against the magnetic field for PQD. By focusing on the Figure obtained we can see that at higher temperature ($T = 70, 90, 100\,K$) the energy decreases as the magnetic field increases, this behavior continues up to a certain value of ω_c, then the energy starts increasing as the magnetic field increases. On the other hand, in the region of low temperatures ($T = 1, 50K$) the energy increases as the magnetic field increases for all values of ω_c.

As the temperature increases, from 1K to 100 K, the average statistical energy curve of the QD shows a great enhancement. This behavior is due to the significant increment in the thermal and the confinement energy contributions.

Figures (3.13, 3.14 and 3.15) show the effect of the confinement frequency ω_0 on the behavior of the curve of the statistical energy $< E >$ against the magnetic field strength ω_c at different temperatures. The Figures show clearly a change in the behaviors of the statistical energy curves as we increase the confinement frequency ω_0 from: 0.5 to1 R^* .

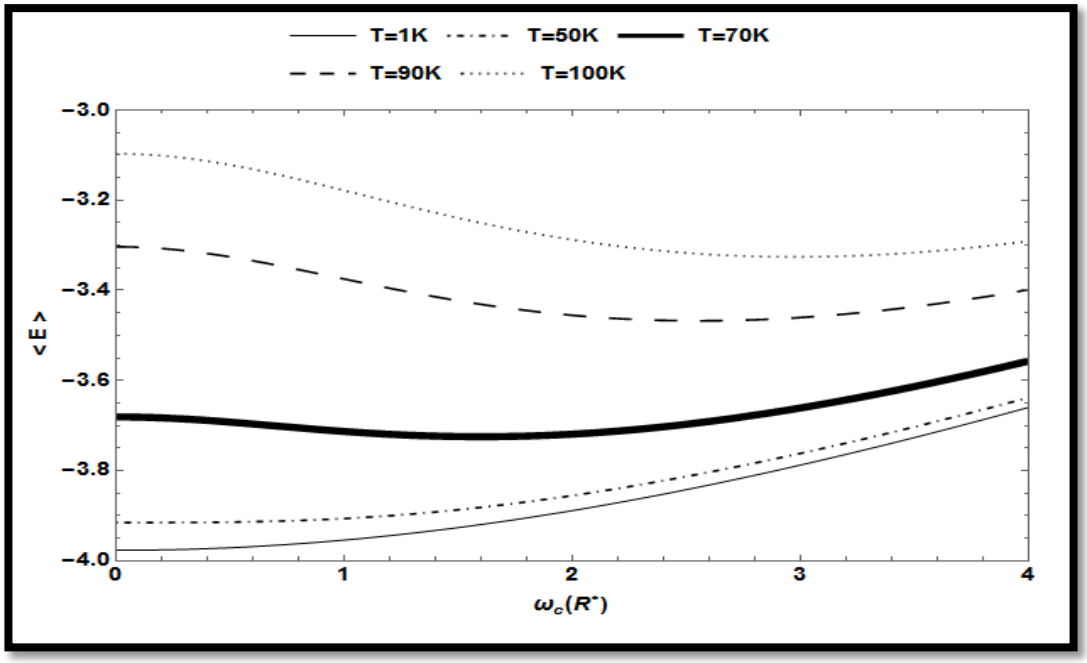

Figure (3.13): The average statistical energy < E > as the function of magnetic field ω_c calculated at ω_0 =0.5 R^* ,$F = 0$ and various temperatures: $T = 1K, 50K$,$70K, 90K$ and $100K$.

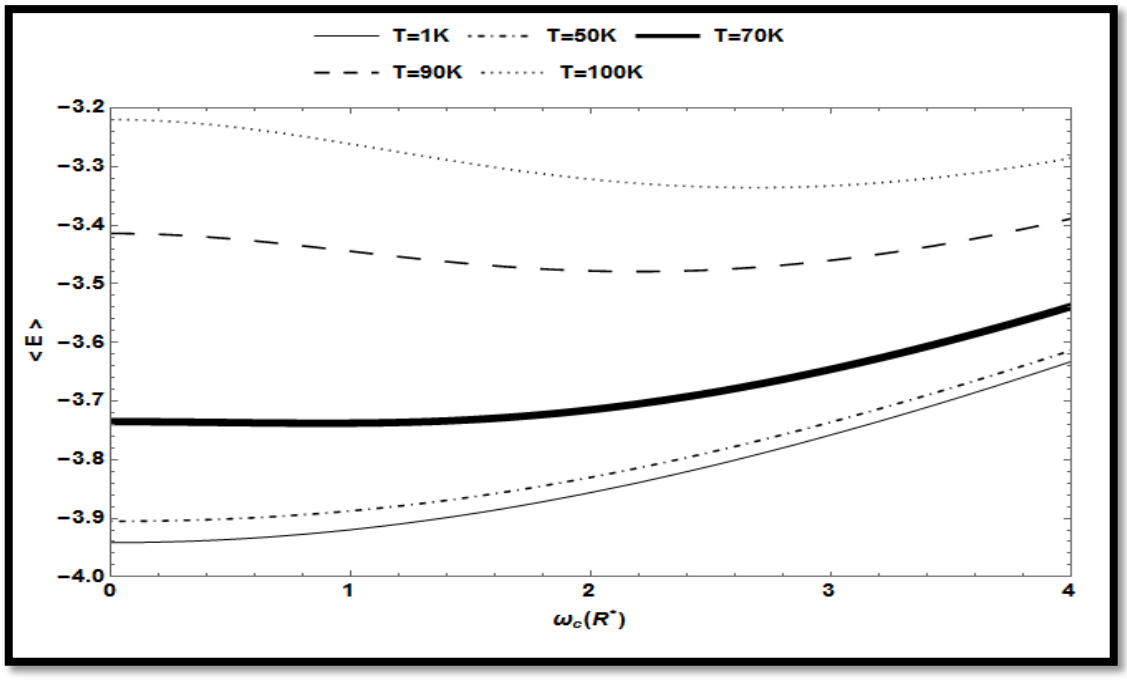

Figure (3.14): The average statistical energy < E > as the function of magnetic field ω_c calculated at ω_0 =0.8 R^* , $F = 0$ and various temperatures $T = 1K, 50K$,$70K, 90K$ and $100K$.

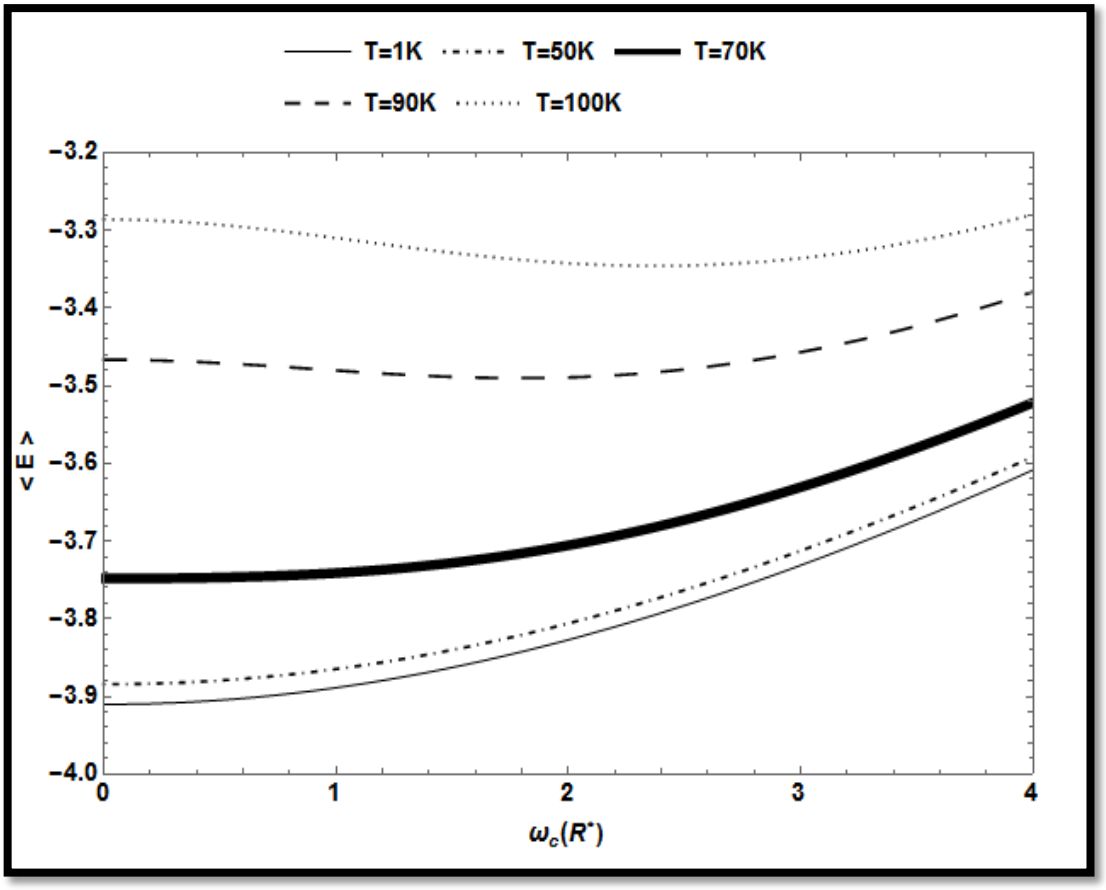

Figure (3.15): The average statistical energy < E > as the function of magnetic field ω_c calculated at ω_0 =1 R^* , F=0 and various temperatures: $T = 1K, 50K, 70K, 90K \text{ and } 100K$.

We plotted in Figure (3.16) the average statistical energy < E > against the magnetic field strength ω_c at different values of electric field F. Calculated at: $T = 10K$ and $\omega_0 = 1.5\ R^*$. The Figure shows obviously that the statistical energy increases as the magnetic field increases for all values of ω_c. Moreover, it can be seen that as the electric field decreases, from 5kV/cm to 0, the average statistical energy curve of the QD shows a great enhancement.

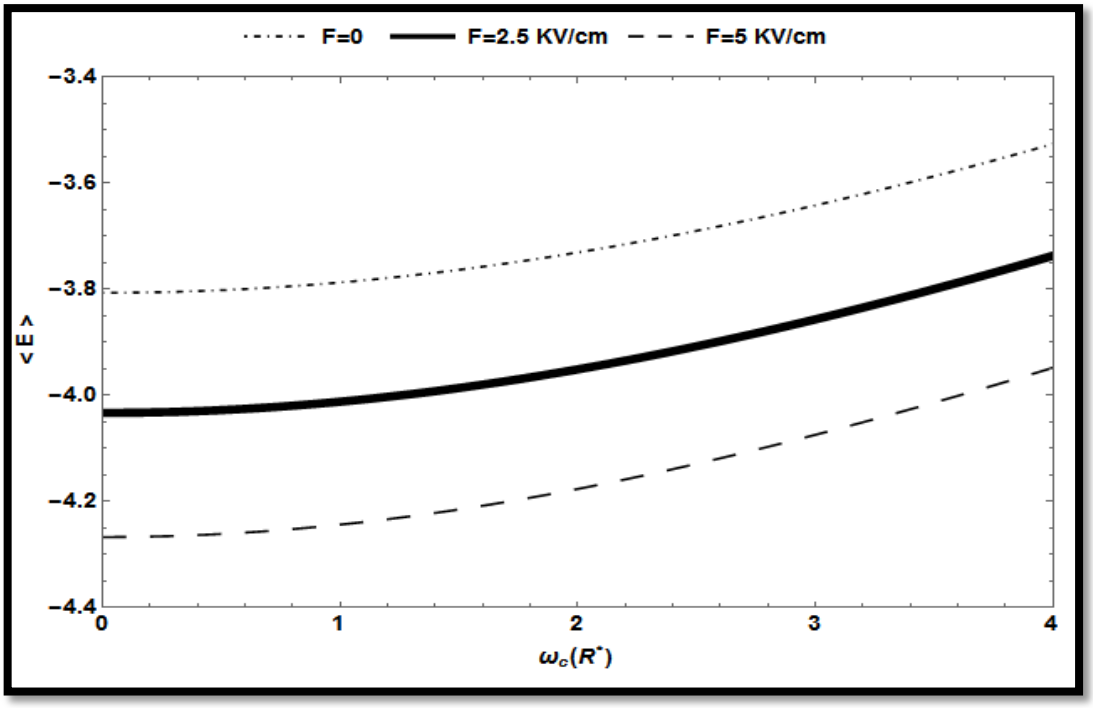

Figure (3.16): The average statistical energy < E> as a function of magnetic field ω_c, calculated at ω_0 =1.5 R^* and various electric field strength: $F = 0, 2.5, 5$ kV/cm and T = 10k.

3.3 Magnetic Properties of the Donor Impurity in Quantum Dot

The second stage in our work is the calculation of the magnetization(M), and the magnetic susceptibility (χ) of a QD as a function of various parameters $(\omega_c,\ \omega_0, T\ and\ F)$.

To study the effect of the presence of donor impurity on the magnetization M, Figures (3.17) and (3.18) show the dependence of the magnetization M upon the magnetic field strength ω_c, for two values of temperature (T), namely $T = 10K$ and $T = 100K$ respectively. It is clear from the Figures that the effect of the impurity is to increase the magnetization M. This is due to the effect of the impurity on the statistical energy behavior as shown in Figures (3.11) and (3.12). For high temperature $T = 100K$, the magnetization in the presence of donor

impurity consequently increases, reaching a peak value then it starts decreasing, while at low temperature $T = 10K$, the magnetization decreases for all values of ω_c, this explain the corresponding magnetic susceptibility (χ) behavior shown in Figures (3.19) and (3.20) for T=10k and T=80k, respectively. It is observed that when $T = 10\ K$ the magnetic susceptibility of the system is negative, which means the system is diamagnetic. On the other hand, for the case $T = 100\ K$ it is found that at a certain value of ω_c the system turns from diamagnetic to paramagnetic.

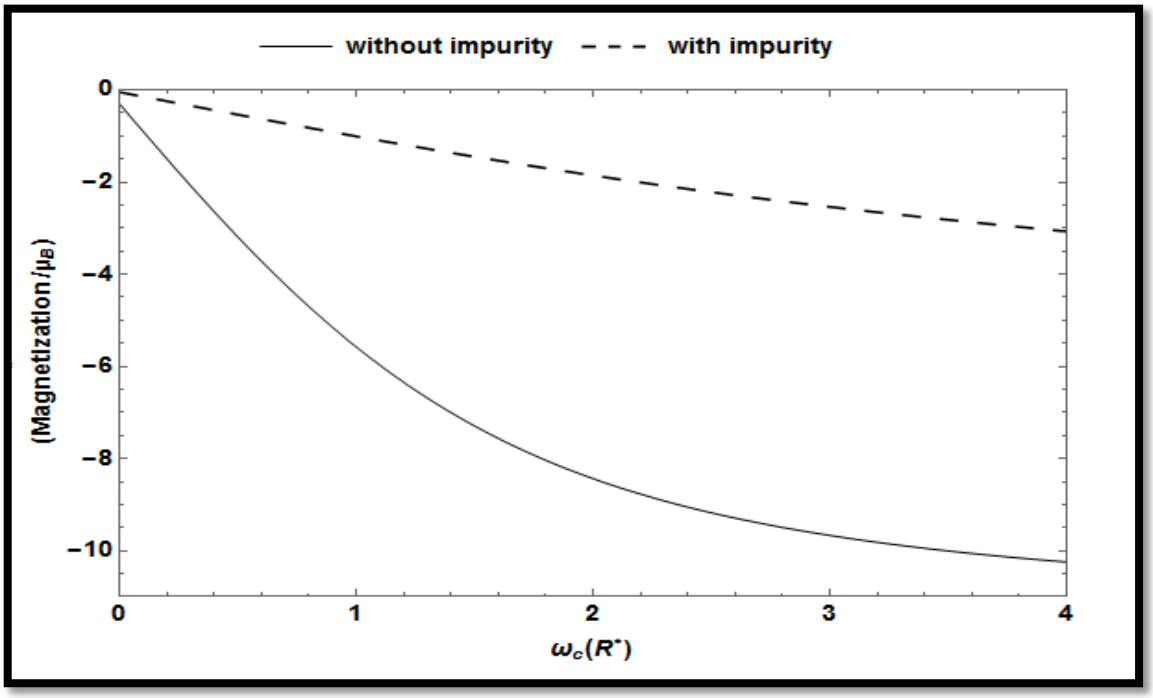

Figure (3.17): The magnetization (in unit of effective Bohr magneton $\mu_B = \frac{e\hbar}{2m^*} = 0.87\ meV/T$ for GaAs) against the magnetic field strengthω_c $(in\ units\ of\ R^*)$, computed at $\omega_0 = 1R^*$, $F = 0$ and $T = 10K$.

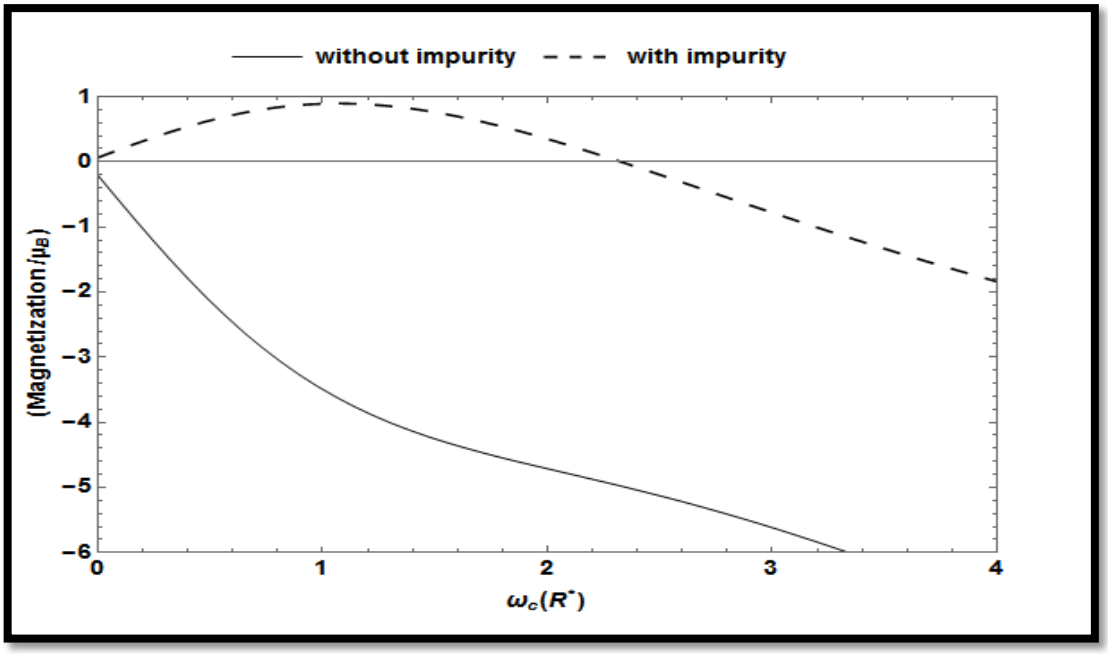

Figure (3.18): The magnetization (in unit of effective Bohr magneton $\mu_B = \frac{e\hbar}{2m^*} = 0.87\ meV/T$ for GaAs) against the magnetic field strength $\omega_c\ (in\ units\ of\ R^*)$, computed at $\omega_0 = 1R^*$, $F = 0$ and $T = 100K$.

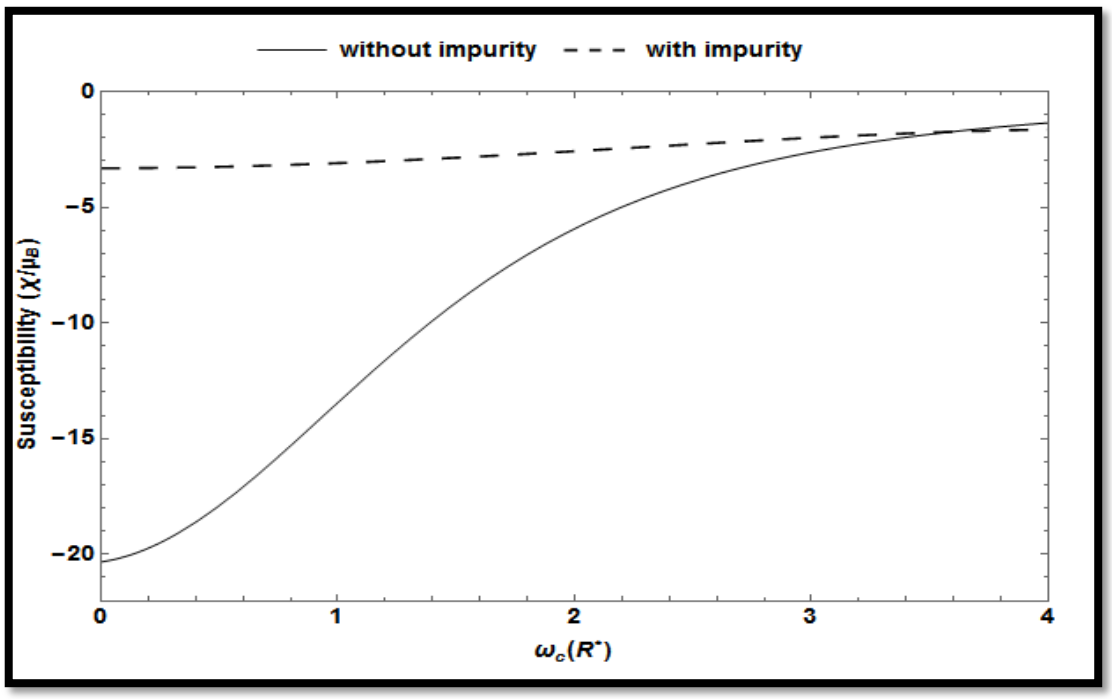

Figure (3.19): The magnetic susceptibility (χ) (in unit of effective Bohr magneto $\mu_B = \frac{e\hbar}{2m^*} = 0.87\ meV/T$ for GaAs) against the magnetic field strength $\omega_c\ (in\ units\ of\ R^*)$ computed at: $\omega_0 = 1R^*, F = 0$ and $T = 10K$.

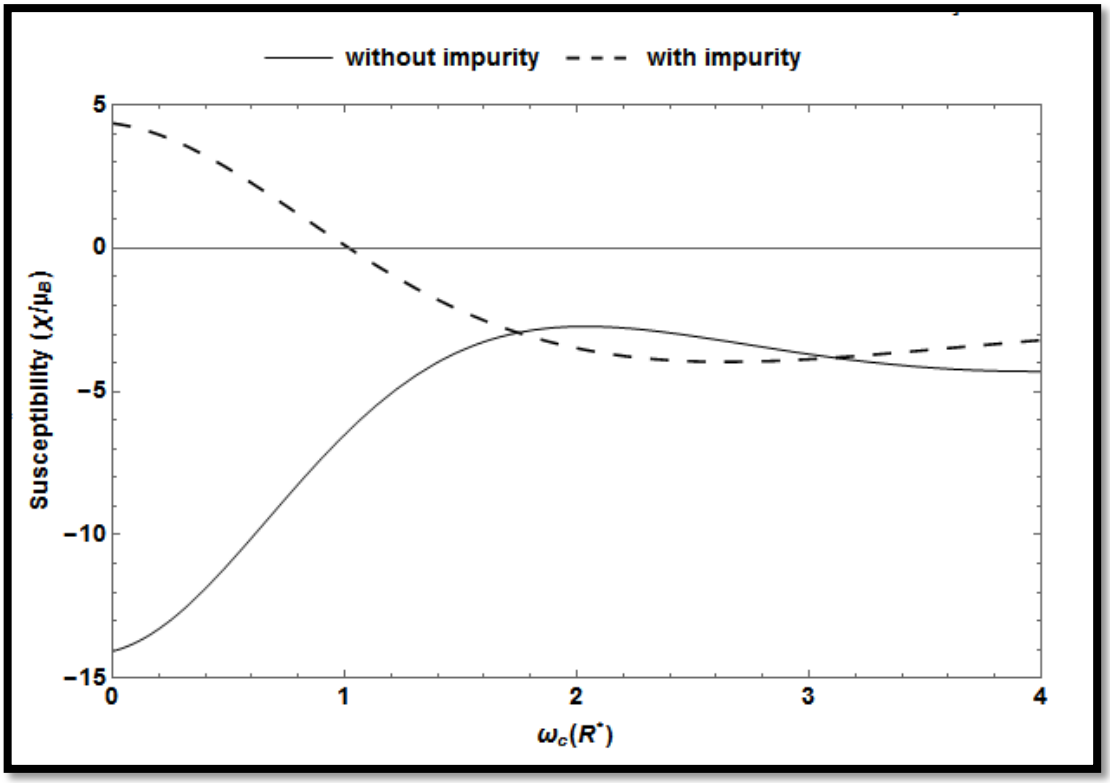

Figure (3.20): The magnetic susceptibility (χ) (in unit of effective Bohr magneto $\mu_B = \frac{e\hbar}{2m^*} = 0.87\ meV/T$ for GaAs) against the magnetic field strength ω_c $(in\ units\ of\ R^*)$ computed at: $\omega_0 = 1R^*, F = 0$ and $T = 100K$.

The variation of the magnetization M in the presence of donor impurity as a function of ω_c at various values of T is shown in Figure (3.21), for fixed value of confinement strength ω_0 and zero electric field. One can observe from the Figure that as the magnetic field ω_c is increased, the magnetization M consequently increases, reaching a peak value then it starts decreasing. Also, the effect of the temperature on the magnetization curve is very significant. As the temperature decreases, the peak value in the magnetization curve decreases and becomes flat for fixed value of ω_0 and F. At a high temperature the thermal energy (E_{th}=K_BT) becomes very significant and in this case it affects greatly the average statistical energy

behavior of the system as shown in Figure (3.13). This leads to a linear increase in the magnetization curve against the magnetic field strength ω_c.

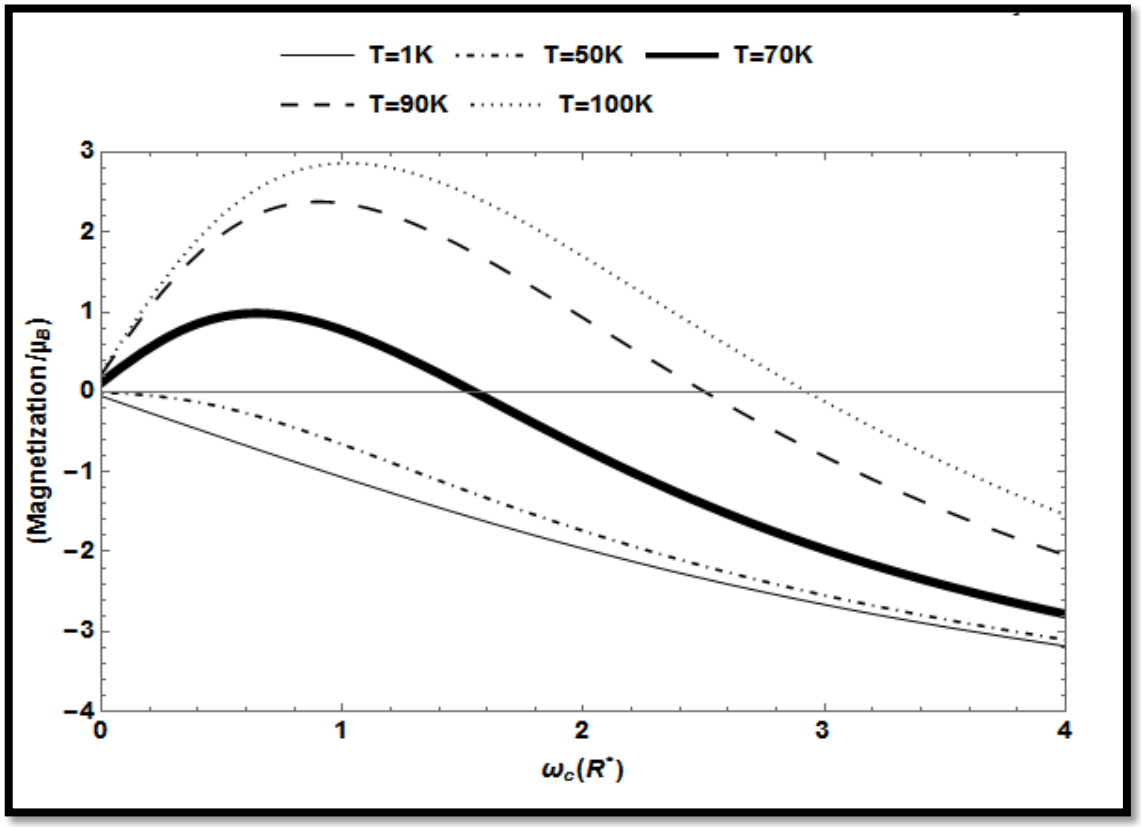

Figure (3.21): The magnetization (in unit of effective Bohr magneton $\mu_B = \frac{e\hbar}{2m^*} = 0.87\ meV/T$ for GaAs) against the magnetic field strength $\omega_c\ (in\ units\ of\ R^*)$, calcualted at $\omega_0 = 0.5R^*$, $F = 0$ and various temperatures: $T = 1K, 50K, 70K, 90K\ and\ 100K$.

In addition, the effect of the confinement frequency ω_0 on the magnetization was also studied by taking different ω_0 values, for example: (ω_0=0.8 R^*) as in Figure (3.22) and (ω_0=1R^*) as in Figure (3.23). By looking at the three Figures (3.21, 3.22 and 3.23), we can notice the effect of changing the confinement frequency ω_0 on the behavior of the magnetization curve at different temperatures. At higher temperatures when the confinement frequency ω_0 increased, the peaks shifted to the left,

towards a lower magnetic field strength and their values decrease and become flat. This is due to the effect of the confinement frequency ω_0 on the statistical energy behavior as shown in Figures: (3.13, 3.14 and 3.15). But at low temperatures the magnetization increase with a relative small amount as the confinement frequency ω_0 increases as seen in Figure (3.24).

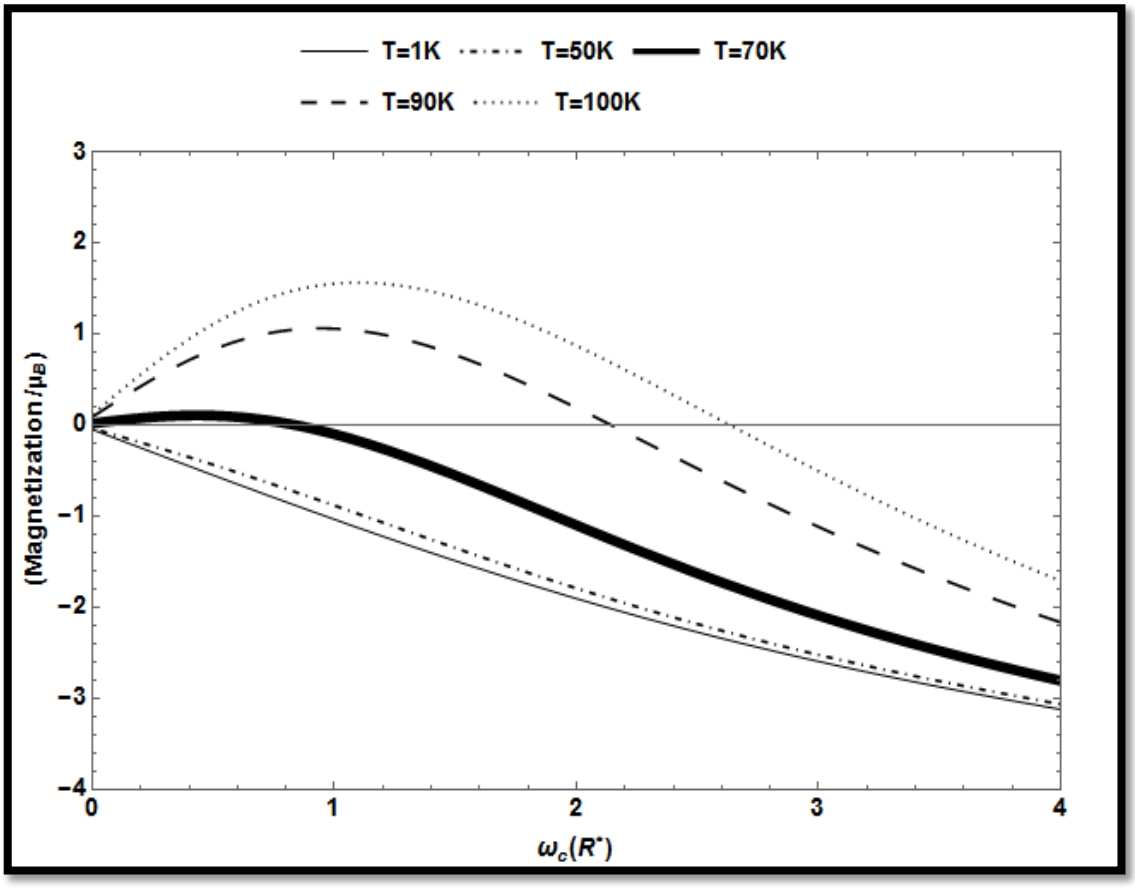

Figure (3.22): The magnetization (in unit of effective Bohr magneton $\mu_B = \frac{e\hbar}{2m^*} = 0.87\ meV/T$ for GaAs) against the magnetic field strength ω_c $(in\ units\ of\ R^*)$, calcualted at $\omega_0 = 0.8R^*$, $F = 0$ and various temperatures: $T = 1K, 50K$,$70K, 90K\ and\ 100K$.

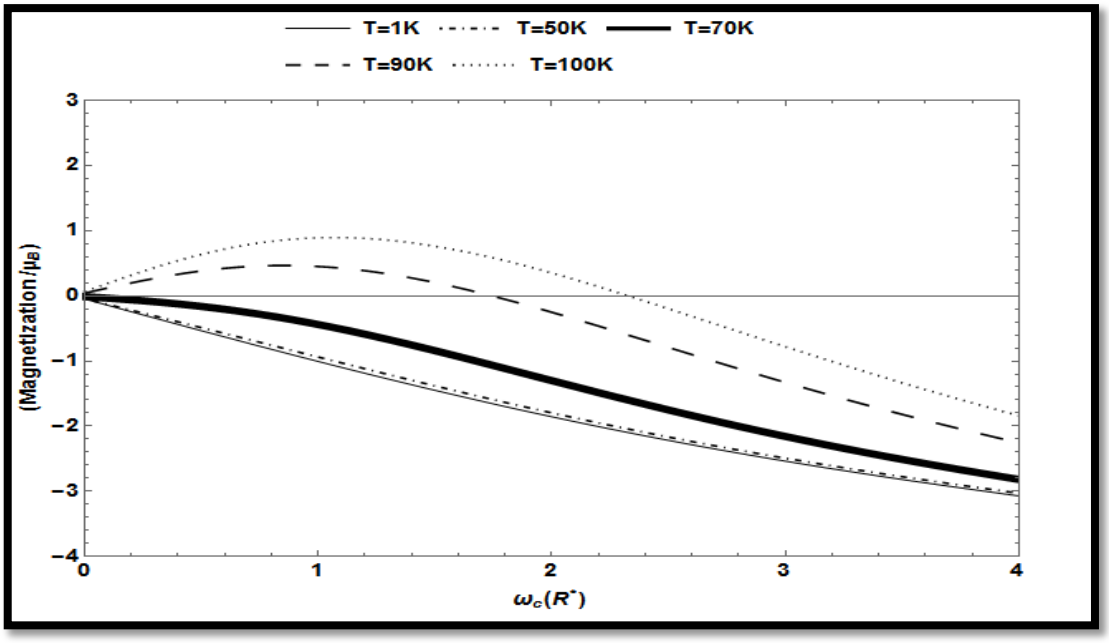

Figure (3.23): The magnetization (in unit of effective Bohr magneton $\mu_B = \frac{e\hbar}{2m^*} = 0.87\ meV/T$ for GaAs) against the magnetic field strength $\omega_c\ (in\ units\ of\ R^*)$, calcualted at $\omega_0 = 1R^*$, $F = 0$ and various temperatures: $T = 1K, 50K, 70K, 90K\ and\ 100K$.

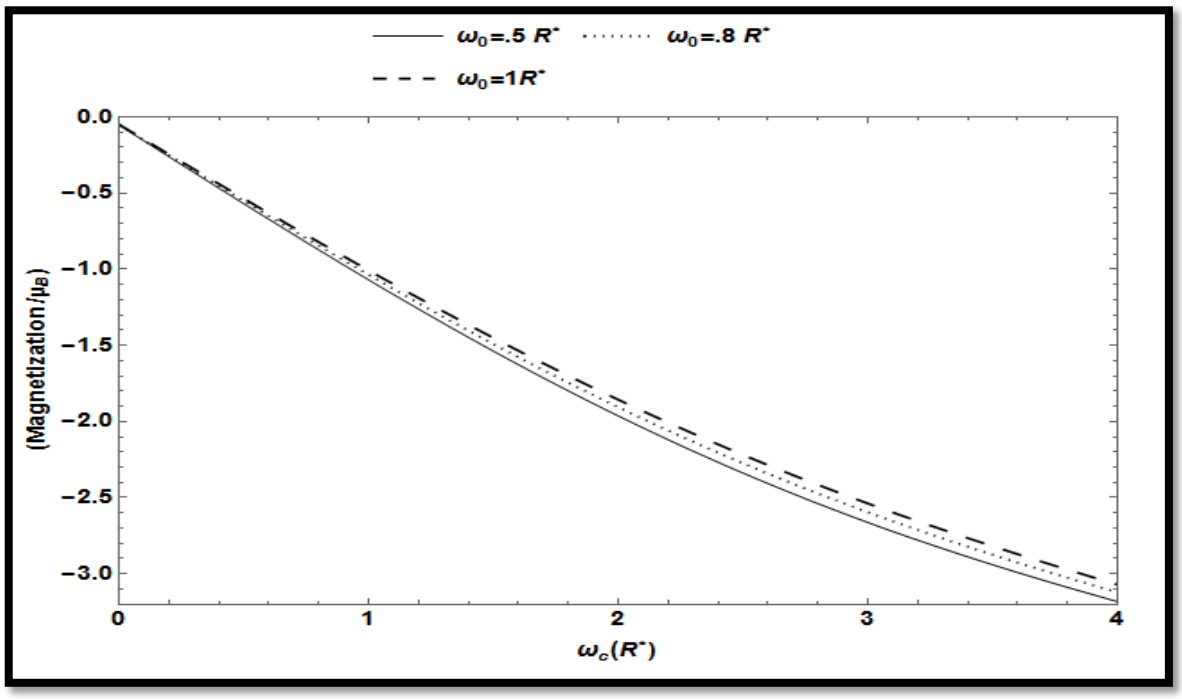

Figure (3.24): The magnetization (in unit of effective Bohr magneton $\mu_B = \frac{e\hbar}{2m^*} = 0.87\ meV/T$ for GaAs) against the magnetic field strength $\omega_c\ (in\ units\ of\ R^*)$, calculated at: $F = 0$, $T = 10K$ and various confinement strengths: $\omega_0 = 0.5\ ,\ 0.8,\ 1R^*$.

Figures 3.25, 3.26 and 3.27 show the corresponding magnetic susceptibility (χ) as a function of the magnetic field strength ω_c at different temperatures. The Figures show clearly great change in the behavior of the magnetic susceptibility curves as we increase the confinement strength ω_0 from 0.5 to 0.8 to 1 R^*. In Figure (3.25) it is observed that for lower values of temperature $(T = 1\ , 50\ K)$ the magnetic susceptibility of the system is negative, which means the system is diamagnetic.

On the other hand, for the higher values of the temperature $(T = 70\ , 90\ , 100\ K)$ it is found that at a certain value of ω_c the magnetic susceptibility (χ) of the donor impurity flips its sign from positive to negative, which means that the system turns from paramagnetic to diamagnetic.

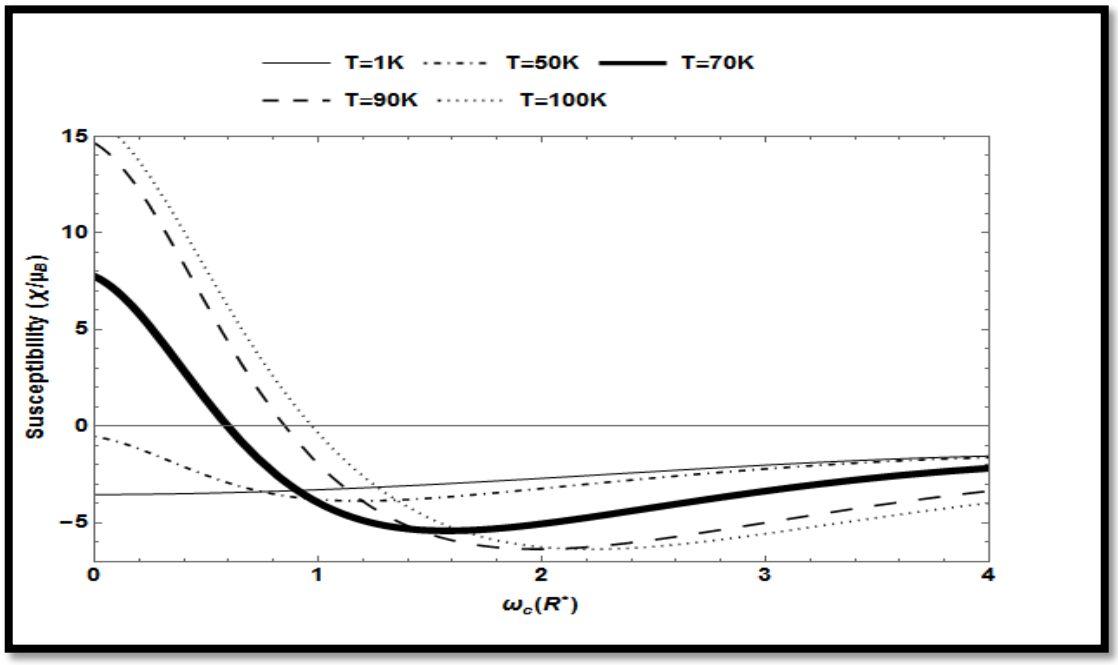

Figure (3.25): The magnetic susceptibility (χ) (in unit of effective Bohr magneton $\mu_B = \frac{e\hbar}{2m^*} = 0.87\ meV/T$ for GaAs) against the magnetic field strength $\omega_c\ (in\ units\ of\ R^*)$, calculated at : $\omega_0 = 0.5\ R^*$, F =0, and various temperatures: $T = 1K, 50K\ ,70K, 90K\ and\ 100K$.

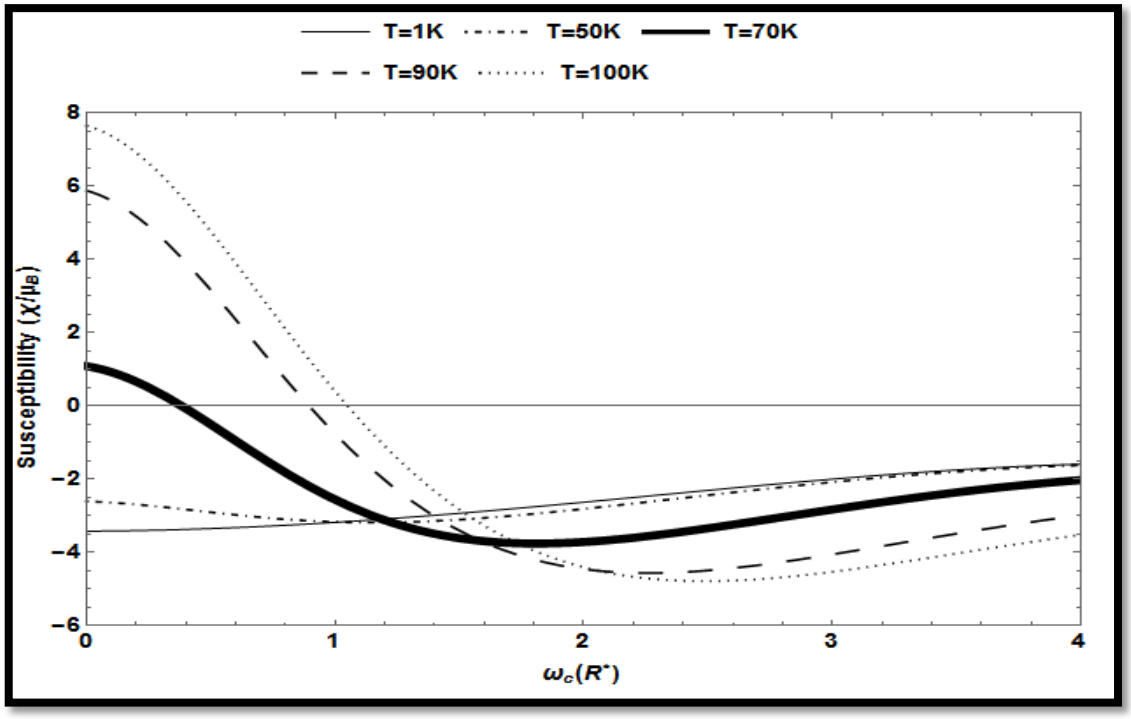

Figure (3.26): The magnetic susceptibility (χ) (in unit of effective Bohr magneton $\mu_B = \frac{e\hbar}{2m^*} = 0.87\ meV/T$ for GaAs) against the magnetic field strength $\omega_c\ (in\ units\ of\ R^*)$, calculated at : $\omega_0 = 0.8\ R^*$, F =0, and various temperatures: $T = 1K, 50K, 70K, 90K\ and\ 100K$.

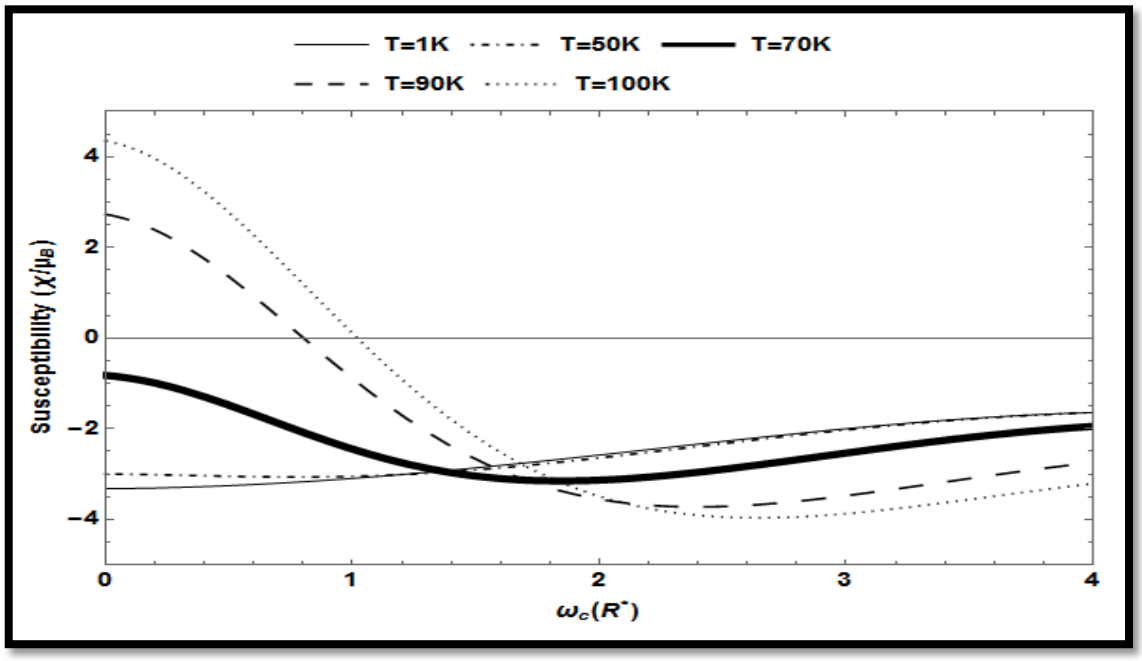

Figure (3.27): The magnetic susceptibility (χ) (in unit of effective Bohr magneton $\mu_B = \frac{e\hbar}{2m^*} = 0.87\ meV/T$ for GaAs) against the magnetic field strength $\omega_c\ (in\ units\ of\ R^*)$, calculated at : $\omega_0 = 1\ R^*$, F =0, and various temperatures: $T = 1K, 50K, 70K, 90K\ and\ 100K$.

In order to understand the dependence of magnetization M upon the electric field strength, the variation of M as a function of ω_c at different values of F is shown in Figure (3.28), it is clear from the figure that the magnetization decrease with increasing$F$, furthermore this Figure shows that the magnetization curve has only negative values, this can attributed to the effect of the electric field strength on the statistical energy behavior as shown in figure (3.16)

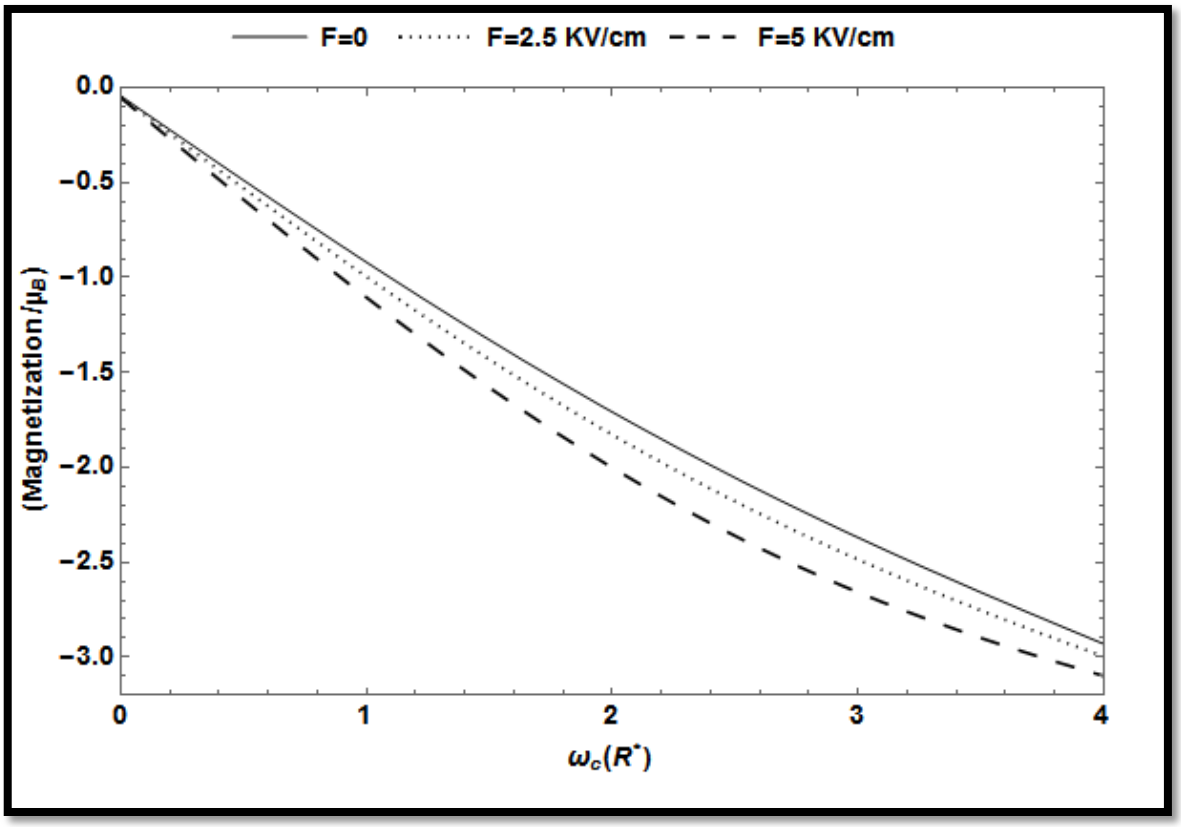

Figure (3.28): The magnetization (in unit of effective Bohr magneton $\mu_B = \frac{e\hbar}{2m^*} = 0.87\ meV/T$ for GaAs) against the magnetic field strength ω_c $(in\ units\ of\ R^*)$, calculated at: $T = 10K$, $\omega_0 = 1.5\ R^*$ and various electric field strength : $F = 0$, 2.5 and 5 kV/cm.

Finally, In order to understand the dependence of magnetic susceptibility (χ) upon the electric field strength F , the variation of χ as a function of ω_c at different values of F is shown in Figure (3. 29), it is clear from the

Figure that as the electric field increases from 0 to 5 kV/cm, the magnetic susceptibility (χ) of the donor impurity flips its sign from negative to positive, which means that the system turns from diamagnetic to paramagnetic.

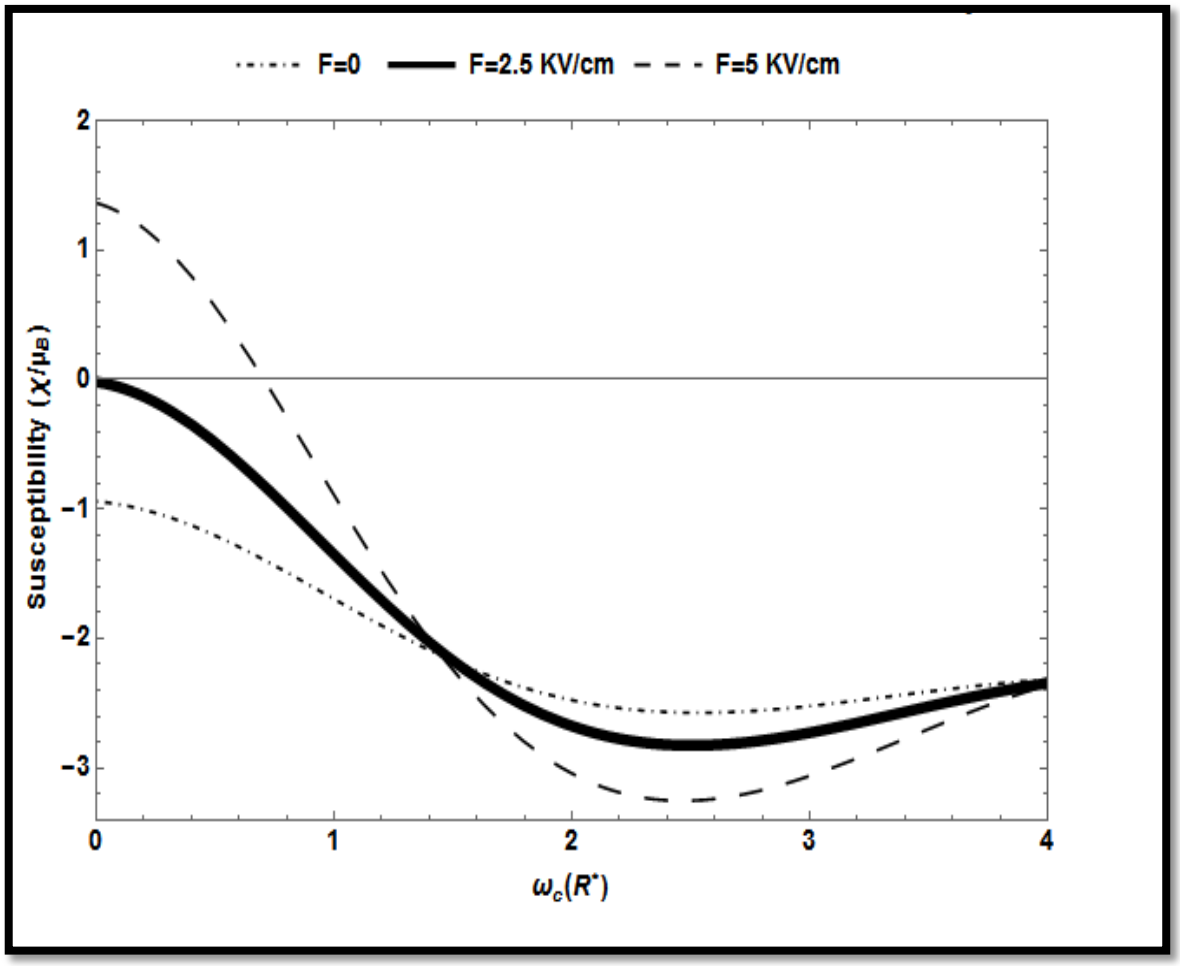

Figure (3.29): The magnetic susceptibility (χ) (in unit of effective Bohr magneton $\mu_B = \frac{e\hbar}{2m^*} = 0.87\ meV/T$ for GaAs) against the magnetic field strength $\omega_c\ (in\ units\ of\ R^*)$, calculated at: $T = 90K$, $\omega_0 = 1.5\ R^*$ and various electric field strength : $F = 0\ , 2.5\ and\ 5\ kV/cm$.

Chapter Four
Conclusions and Future Work

In conclusion, using the shifted 1/N expansion method, we have studied the energies and binding energies of an electron bound to an on center impurity confined in a parabolic two dimensional quantum dot. Then the effects of externally applied magnetic and electric fields have been investigated for the ground state and low-lying excited states, our results show that the donor impurity energy and binding energy depends strongly on the confinement strength ω_0, magnetic field strength ω_c, and electric field strength F. The dependence can be summarized as follows : the donor impurity energy and binding energy increase with increasing the confinement strength ω_0. Moreover, the confinement effects enhance (reduce) and then the energy and the binding energy increase(decrease) with increasing external applied magnetic (electric)field.

We have next studied the magnetization and the magnetic susceptibility of a donor impurity in quantum dot, it has been observed that the effect of the impurity is to increase the magnetization M. Also, the magnetization and the magnetic susceptibility were calculated as function of the magnetic field strength (ω_c) at different values of the temperature(T), confinement strength ω_0 and electric field strength F. The computed results allowed us to study the effect of the confinement strength ω_0 and the temperature (T) on the behavior of the peaks in the magnetization curves. And then on the corresponding magnetic susceptibility, it is found that at a certain values of ω_c , T and F the system turns from paramagnetic to diamagnetic.

In this work the impurity presence, the confinement strength ω_0 , the externally applied magnetic and electric fields effects on the energy and binding energy has been studied. Also the magnetization and the magnetic susceptibility had been investigated as a magnetic property of the QD system. The electronic, thermodynamic and magnetic properties of donor impurities in quantum dot are very interesting issues duo to their potential device applications. This hot research topic requires further investigations in the future.

References

[1] S. Dey, D. Swargiary, D. Dasgupta, D. Bordoloi, R. Saikia, D. Neog, ... & S. Choudhury. **The confinement energy of quantum dots,** arXiv preprint arXiv. **1212**, 2318 (2012).

[2] A. P. Alivisatos. ***Perspectives on the physical chemistry of semiconductor nanocrystals,*** **J. Phys Chem**. **100**, 13226 (1996).

[3] R. Rossetti, L. Brus. ***Electron-hole recombination emission as a probe of surface-chemistry in aqueous CdS colloids***, **J. Phys. Chem**. 86, 4470 (1982).

[4] W. J. Parak, L.Manna and Th. Nann. **Fundamental principles of quantum dots**, Nanotechnology. **1,** 75(2008).

[5] J. H. Davies. **The Physics of Low dimensional Semiconductors**, Cambridge University Press (1998).

[6] T. Ando, A. B. Fowler, and F. Stern. **Electronic properties of two-dimensional systems**, Reviews of Modern Physics. **54(2),** 437 (1982).

[7] G. Moody. **Effects on the electronic and optical properties of semiconductor quantum dots revealed with two-dimensional coherent spectroscopy**, Ph. D. Thesis, University of Colorado (2013).

[8] E. O. Chukwuocha, M. C. Onyeaju and T. S. Harry. ***Theoretical studies on the effect of confinement on quantum dots using the brus equation***, **World Journal of Condensed Matter Physics**. **2(02)**, 96 (2012).

[9] M. A. Reed, E. S. Hornbeck, M. R. Deshpande, R. G. Wheeler, R. C. Bowen, J. N. Randal and W. R. Frensley. **Quantum Dots**, Scientific American. **268(1),** 118 (1993).

[10] C. Wang, M. Shim and P. Guyot-Sionnest. **Electrochro-mic Nanocrystal Quantum Dots,** Science. 291, 2390(2001).

[11] E. Petryayeva, W. R. Algar and I. L. Medintz. **Quantum dots in bioanalysis: a review of applications across various platforms for fluorescence spectroscopy and imaging**, applied spectroscopy. **67(3),** 215 (2013).

[12] A. A. Lagatsky, C. G. Leburn, C. T. A. Brown, W. Sibbett, S. A. Zolotovskaya and E. U. Rafailov. **Ul-trashort pulse lasers passively mode Locked by quantum dot based saturable absorbers**, Progress in Quantum Electronics. 34(1), 1(2010).

[13] R. Koole, E. Groeneveld, D. Vanmaekelbergh, A. Meijerink and, C. de Mello Donegá. **Size effects on semiconductor nanoparticles**, Nanoparticles, Berlin, Heidelberg, 13(2014).

[14] F. M. Bzour. **Effects of the hydrostatic pressure and temperature on the properties of the (GaAs) single quantum dot in a magnetic field,** M. Sc Thesis, An-Najah National University (2016).

[15] P. O. nikeeva, J. E. Halpert, M. G. Bawendi and V. Bulovic. **Quantum dot light-emitting devices with electroluminescence tunable over the entire visible spectrum**, Nano letters. ***9*(7),** 2532 (2009).

[16] L. Kim, P. Anikeeva, S. Coe-Sullivan, J. Steckel, M. Bawendi, and V. Bulović**. Contact Printing of Quantum Dot Light-Emitting Devices**, Nano Letters. **8 (12),** 4513 (2008).

[17] G. Bastard. **Exciton binding energy in quantum wells**, Phys. Rev. B 59, 4714(1981).

[18] M. K. Bose, K. Midya and C. Bose. ***Effect of polarization and self-energy on the ground donor state in the presence of conduction band nonparabolicity in GaAs–(Al, Ga) as spherical quantum dot,*** **Journal of Applied Physics**. **101**, 054315(2007).

[19] I. F. I. Mikhail, I. M. M. Ismail. **Binding energy of an off-center hydrogenic donor impurity in a spherical quantum dot**, Physica Status Solidi. **B 244,** 3647 (2007).

[20] M. Barati, G. Rezaei, M. R. K. Vahdani. **Binding energy of a hydrogenic donor impurity in an ellipsoidal finite-potential quantum dot,** Physica Status Solidi**. B 244,** 2605(2007).

[21] R.S. Daries Bella, K. Navaneethakrishnan. **Donor binding energies and spin–orbit coupling in a spherical quantum dot**, Solid State Communications. **130**, 773 (2004).

[22] R. Kostic and D. Stojanovic. ***Electric field effect on the nonlinear and linear intersubband absorption spectra in CdTe/ZnTe spherical quantum dot***, **Journal of Nanophotonics**. **6(1)**, 061606 (2012).

[23] N. Porras-Montenegro and S. T. Pe´rez-Merchancano. **Hydrogenic impurities in GaAs-(Ga,Al)As quantum dots**, Phys. Rev. B 46, 9780 (1992).

[24] J. L. Zhu, J. J. Xiong and B. L. Gu. **Confined electron and hydrogenic donor states in a spherical quantum dot of GaAs-Ga 1− x Al x As**, Phys. Rev**.** B 41**,** 6001 (1990).

[25] W. F. Xie. **Binding energy of an off-center hydrogenic donor in a spherical Gaussian quantum dot,** Physica. B 403**,** 2828 (2008).

[26] J. L. zhu, X. Chen. **Spectrum and binding of an off-center donor in a spherical quantum dot**, Phys. Rev. B 50, 4497(1994).

[27] S. T. Pérez-Merchancano, L. E. Bolivar-Marinez and J.Silva-Valencia**. The binding energy of donor impurities in GaAs quantum dots under the pressure effect**, Revista mexicana de física. **53(6)**, 470 (2007).

[28] A. Kumar, S. E. Laux and F. Stern. **Electron states in a GaAs quantum dot in a magnetic field,** Phys. Rev**. B 42,** 5166 (1990).

[29] M. G. Barseghyan, A. A. Kirakosyan and C. A. Duque. ***Donor-impurity related binding energy and photoinization cross-section in quantum dots: electric and magnetic fields and hydrostatic pressure effects***, **The European Physical Journa**. **B72 (4),** 521(2009).

[30] S. Baskoutas, E. Paspalakis and A. F. Terzis. ***Electronic structure and nonlinear optical rectification in a quantum dot: effects of impurities and external electric field***, **Journal of Physics: Condensed Matter**. **19(39),** 395024 (2007).

[31] M. G. Barseghyan, A. Hakimyfard, A. A. Kirakosyan, M. E. Mora-Ramos and C. A. Duque. **Hydrostatic pressure and electric and magnetic field effects on the binding energy of a hydrogenic donor impurity in InAs Pöschl–Teller quantum ring**, Superlattices and Microstructure. **51 (1)**, 119 (2012).

[32] M. Elsaid. **Effects of applied magnetic field on the energy levels of shallow donors in a parabolic quantum dot,** Physica. B 202**,** 202(1994) .

[33] Z. Zeng, G. Garoufalis, and S. Baskoutas. **Competition effects of electric and magnetic fields on impurity binding energy in a disc-shaped quantum dot in the presence of pressure and temperature,** Science of Advanced Materials. **6(3)**, 586 (2014).

[34] A. John peter, K. Gnanasekar, K. Navaneethakrishnan. ***Combined effects of electric and magnetic fields on confined donor states in a diluted magnetic semiconductor parabolic quantum dot,*** **The European Physical Journal B-Condensed Matter and Complex Systems**, **B 53(3)**, 283(2006).

[35] G. Rezaei, S. Kish. **Effects of external electric and magnetic fields, hydrostatic pressure and temperature on the binding energy of a hydrogenic impurity confined in a two-dimensional quantum dot,** Physica E: Low-dimensional Systems and Nanostructures, **45**, 56 (2012).

[36] A. Boda and A. Chatterjee. **Transition energies and magnetic properties of a neutral donor complex in a Gaussian GaAs quantum dot**. Superlattices and Microstructures, **97**, 268(2016).

[37] Z. Hong, Z. Li-Xue, W. Xue, Z.Chun-Yuan and L. Jian-Jun. **Impurity-related electronic properties in quantum dots under electric and magnetic fields**, Chinese Physics B, **B20(3)**, 037301(2011).

[38] J. H. Yuan, Y. Zhang, X. Guo, J. Zhang, and H. Mo. **The low-lying states and optical absorption properties of a hydrogenic impurity in a parabolic quantum dot modulation by applied electric field**. Physica E: Low-dimensional Systems and Nanostructures, **68**, 232 (2015).

[39] F. M. Bzour. **Effects of the hydrostatic pressure and temperature on the properties of the (GaAs) single quantum dot in a magnetic field,** M. Sc Thesis, An-Najah National University (2016).

[40] A. Shaer. **Heat capacity of two electrons quantum dot in an external magnetic field by variational method,** M. Sc Thesis, An-Najah National University (2015).

[41] E. Hjaz, M. K. Elsaid, M. Elhasan**.** ***Magnetization of coupled double quantum dot in magnetic fields***, **Journal of Computational and Theoretical Nanoscience**, **14(4),** 1700 (2017).

[42] F. Bzour, M. K. Elsaid, A . Shaer. **The Effects of pressure and temperature on the magnetic susceptibility of semiconductor quantum dot in a magnetic field**, Applied Physics Research, **9(1)**, 77 (2017).

[43] M. Elsaid, E. Hijaz. **Magnetic susceptibility of coupled double GaAs quantum dot in magnetic Fields**, Acta Physica Polonica, **131**, 1491 (2017).

[44] M. Elsaid, E. Hjaz, A. Shaer. ***Energy states and exchange energy of coupled double quantum dot in a magnetic field***, **International Journal of Nano Dimension** , **8**,1 (2017).

[45] A. Shaer, M. K. Elsaid, M. Elhasan. ***Variational calculations of the heat capacity of a semiconductor quantum dot in magnetic fields***, **Chinese Journal of Physics**, **54**, 3 (2016).

[46] A. Shaer, M.K. Elsaid, M. Elhasan. ***Magnetization of GaAs parabolic quantum dot by variation method***, **Journal of Physical Science and ApplicationJ**, **6**, 39 (2016)

Appendix

Shifted 1/N Expansion Method

If Eq.7 expands around (r_0) one has:

$$[-\frac{d^2}{dx^2}+\frac{\bar{k}}{4}\left(1+\frac{3x^2}{\bar{k}}-\frac{4x^3}{\bar{k}^{3/2}}+\frac{5x^4}{\bar{k}^2}-\cdots\right)-\frac{(2-a)}{2}\left(1-\frac{2x}{\bar{k}^{1/2}}+\frac{3x^2}{\bar{k}}-\cdots\right)$$
$$+\frac{(1-a)(3-a)}{4\bar{k}}\left(1-\frac{2x}{\bar{k}^{1/2}}+\frac{3x^2}{\bar{k}}-\cdots\right)+\frac{r_0^2\bar{k}}{Q}(V(r_0)+\frac{V''(r_0)r_0^2x^2}{2\bar{k}}+$$
$$\frac{V'''(r_0)r_0^3x^3}{6\bar{k}^{3/2}}+\cdots)]\,\phi(r)=\frac{Er_0^2}{\bar{k}}\,\phi(r) \qquad \text{(A1)}$$

The Schrodinger equation for one - dimensional anharmonic oscillator is given as:

$$[-\frac{d^2}{dx^2}+\frac{1}{4}\omega^2x^2+\epsilon_0+V(x)]\,\phi(x)=\lambda\,\phi(x) \qquad \text{(A2)}$$

Where the perturbation $V(x)$ is given by:

$$V(x)=g^{1/2}(\epsilon_1x+\epsilon_3x^3)+g(\epsilon_2x^2+\epsilon_4x^4)+g^{3/2}(\delta_1x+\delta_3x^3+$$
$$\delta_5x^5)+\,g^2(\delta_2x^2+\delta_4x^4+\delta_6x^6) \qquad \text{(A3)}$$

We can compare Eqs. (A1) and (A2) term by term to define all the anharmonic Parameters in terms of $\bar{k}$, Q, r_0 and the potential derivatives.

Proceeding in a straightforward way we obtain the following identifications:

$$\omega=\left[3+\frac{2r_0^4V''(r_0)}{Q}\right]^{1/2}=\left[3+\frac{r_0V''(r_0)}{V'(r_0)}\right]^{1/2} \qquad \text{(A4)}$$

$$g=\frac{1}{\bar{k}}\,,\qquad \lambda=\frac{Er_0^2}{\bar{k}}$$

$$\epsilon_0=\frac{\bar{k}}{4}-\frac{(2-a)}{2}+\frac{(1-a)(3-a)}{4\bar{k}}+\frac{r_0^2\bar{k}}{Q}V(r_0) \qquad \text{(A5)}$$

$\epsilon_1 = (2-a)$, $\epsilon_2 = \frac{-3}{2}(2-a)$, $\epsilon_3 = -1 + \frac{r_0 V'''(r_0)}{6Q}$

$\epsilon_4 = \frac{5}{4} + \frac{r_0^6 V''''(r_0)}{24Q}$, $\delta_1 = -\frac{(1-a)(3-a)}{2}$, $\delta_2 = \frac{(1-a)(3-a)}{4}$

$\delta_3 = 2(2-a)$, $\delta_4 = -\frac{5(2-a)}{2}$, $\delta_5 = \frac{-3}{2} + \frac{r_0^7 V'''''(r_0)}{120Q}$,

$\delta_6 = \frac{7}{4} + \frac{r_0^8 V''''''(r_0)}{720Q}$

For any value of n_r (radial quantum number) and for any value of m_l , the energy $E\ (n_r\ , m_l)$ is given by an expression in powers of $1/\bar{k}$ (up to third order) as:

$E = E_0 + E_1 + E_2 + E_3$

Where

$E_0 = \bar{k}^2[\frac{1}{4r_0^2} + \frac{V(r_0)}{Q}]$

$E_1 = \frac{\bar{k}}{r_0^2}[\left(n_r + \frac{1}{2}\right)\omega - \frac{(2-a)}{2}]$

$E_2 = \frac{1}{r_0^2}[\frac{1}{4}(1-a)(3-a) + \{(1+2n_r)\tilde{\epsilon}_2 + 3\tilde{\epsilon}_4(1+2n_r+2{n_r}^2)\} - \frac{1}{\omega}\{\tilde{\epsilon}_1 + 6(1+2n_r)\tilde{\epsilon}_1\tilde{\epsilon}_3 + (11+30n_r+30{n_r}^2)\tilde{\epsilon}_3^2\}]$

$E_3 = \frac{1}{\bar{k}r_0^2}[\{(1+2n_r)\,\tilde{\delta}_2 + 3(1+2n_r+2{n_r}^2)\tilde{\delta}_4 + 5(3+8n_r+6{n_r}^2 + 4{n_r}^3)\tilde{\delta}_6\} - \frac{1}{\omega}\Big\{(1+2n_r)\tilde{\epsilon}_2^2 + 12(1+2n_r+2{n_r}^2)\tilde{\epsilon}_2\tilde{\epsilon}_4 + 2(21 + 59n_r + 51{n_r}^2 + 34{n_r}^3)\tilde{\epsilon}_4^2 + 2\tilde{\epsilon}_1\tilde{\delta}_1 + 6(1+2n_r)\tilde{\epsilon}_1\tilde{\delta}_3 + 30(1+2n_r + 2{n_r}^2)\tilde{\epsilon}_1\tilde{\delta}_5 + 6(1+2n_r)\tilde{\epsilon}_3\tilde{\delta}_1 + 2(11+30n_r+30{n_r}^2)\tilde{\epsilon}_3\tilde{\delta}_3 + 10(13 + 40n_r + 42{n_r}^2 + 28{n_r}^3)\tilde{\epsilon}_3\tilde{\delta}_5\} + \frac{1}{\omega^2}\{4\tilde{\epsilon}_1^2\tilde{\epsilon}_2 + 36(1+2n_r)\tilde{\epsilon}_1\tilde{\epsilon}_2\tilde{\epsilon}_3 + 8(11+30n_r+30{n_r}^2)\tilde{\epsilon}_2\tilde{\epsilon}_3^2 + 24(1+2n_r)\tilde{\epsilon}_2^2\tilde{\epsilon}_4 + 8(31+78n_r + 78{n_r}^2)\tilde{\epsilon}_1\tilde{\epsilon}_3\tilde{\epsilon}_4 + 12(57+189n_r+225{n_r}^2+150{n_r}^3)\tilde{\epsilon}_3^2\tilde{\epsilon}_4\Big\}$

$$+\ \frac{1}{\omega^3}\{8\tilde{\epsilon}_1^2\tilde{\epsilon}_3 + 108(1+2n_r)\tilde{\epsilon}_1^2\tilde{\epsilon}_3^2 + 48(11+30n_r+30{n_r}^2)\tilde{\epsilon}_1\tilde{\epsilon}_3^3 + 30(31+109n_r+141{n_r}^2+94{n_r}^3)\,\tilde{\epsilon}_3^4)$$

Where

$$\tilde{\epsilon}_j = \frac{\epsilon_j}{\omega^{j/2}},\quad \tilde{\delta}_j = \frac{\delta_j}{\omega^{j/2}}\ , j = 1,2,3, \ldots \ldots \text{j}$$

جامعة النجاح الوطنية

كلية الدراسات العليا

تأثير المجالين المغناطيسي والكهربائي على مستويات الشوائب المانحة في نقطه كميه مصنوعه من ماده GaAs

إعداد

أسماء زهير مدحت ياسين

إشراف

أ.د. محمد السعيد

د. موسى الحسن

قدمت هذه الأطروحة استكمالاً لمتطلبات الحصول على درجة الماجستير في الفيزياء، بكلية الدراسات العليا، في جامعة النجاح الوطنية، نابلس – فلسطين.

2018

تأثير المجالين المغناطيسي والكهربائي على مستويات الشوائب المانحة في نقطه كميه مصنوعه من ماده GaAs

إعداد

اسماء زهير مدحت ياسين

إشراف

أ.د. محمد السعيد

د. موسى الحسن

الملخص

في هذا العمل تم حساب طاقه المستوى الارضي وبعض المستويات العلوية للشوائب المانحة المحصورة في نقطه كميه مصنوعه من ماده GaAs تحت تأثير كل من المجالين المغناطيسي والكهربائي، وذلك عن طريق حل دالة هاملتون بطريقة مفكوك (1/N)، بالإضافة الى حساب طاقه الربط لتلك المستويات. لقد قمنا بدراسة التأثير المشترك للمجال الكهربائي والمغناطيسي على طاقه المستويات وعلى طاقه الربط، وكانت النتيجة بانه مع زياده شده المجال المغناطيسي فان طاقه المستويات وكذلك طاقه الربط تزداد، اما بالنسبة للمجال الكهربائي فان الطاقة وطاقه الربط لتلك المستويات تقل. وفيما بعد قمنا بدراسة الخصائص المغناطيسية لتلك النقطة الكميه من خلال دراستنا للتمغنط وكذلك قابليه التمغنط وتم فحص اعتماد كمية التمغنط وقابليه التمغنط على كل من المتغيرات التالية: درجة الحرارة والمجال المغناطيسي وجهد الحصر والمجال الكهربائي، اظهرت المقارنات المعروضة في الاطروحة تطابقا كبيرا بين النتائج التي حصلنا عليها مع الاعمال المنشورة.